

## Response to Reviewer 1 (Britt Stephens).

We thank Dr. Stephens for his helpful and very detailed comments. His major comments are reprinted here in blue and our responses are given in black. Below, we also provide a list of responses to the minor comments in his annotated PDF file.

This paper applies observations of seasonal cycles in atmospheric oxygen to evaluate a subset of ocean biogeochemistry models participating in the CMIP5 project and uses satellite-based productivity estimates to derive complementary insights. It is a nice demonstration of the applicability of oxygen data to this task and provides useful insights into the behavior of recent models relative to observations and other models. Although productivity estimates from space are highly uncertain, the paper shows that phasing information makes an additional contribution. The use of matrixed response functions from TransCom3 era uniform flux simulations to link the models and observations is not optimal, but I recommend publication with only modest revisions. Major comments are below, while minor suggestions are made inline in the attached pdf.

### Major comments

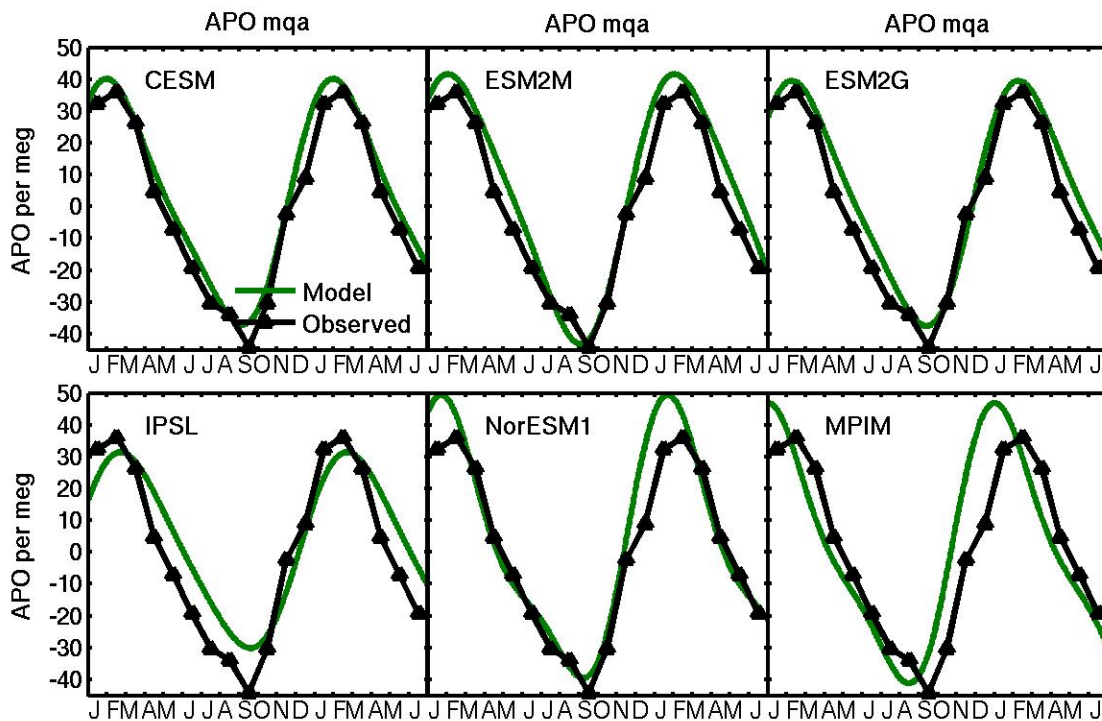
1) The authors use atmospheric transport simulation output from the TransCom 3 Level 2 experiment to translate ocean model fluxes into estimated atmospheric signals. These model runs were conducted about 13 years ago and there have been significant advances in atmospheric transport model resolution and fidelity since then. Furthermore these runs were done using uniform flux distributions and as the authors show, this leads to considerable differences with respect to O<sub>2</sub> specific patterns. If I were associated with one of the ocean models that doesn't look very good in this analysis, I would be tempted to insist that the analysis be redone with modern atmospheric transport models and O<sub>2</sub> flux patterns. Independent atmospheric transport models have also converged significantly in the past decade, and using the TransCom model spread as an estimate of uncertainty here may undersell the potential for atmospheric O<sub>2</sub> data to test ocean models. For example, the standard deviation on northern extratropical land fluxes, which has been linked to differences in vertical mixing, shrunk by over a factor of 2 from the TransCom 3 Level 2 study (Gurney et al., GBC 2004) and the RECCAP study (Peylin et al., BG, 2013), and the RECCAP study allowed different methodologies and observational networks suggesting transport has converged even further. Of course, the right thing to do would be to collaborate with atmospheric transport modeling groups to run O<sub>2</sub> flux patterns through modern transport models. Using these old matrixed response functions, which as the authors point out can be run in seconds, seems somewhat to be taking the easy way out. Nonetheless, the approach and results presented here are sufficiently well defended for publication. I would however suggest adding discussion of the dated nature of these simulations and the possibilities of bias and/or overestimated uncertainty. I would also encourage the authors to use more rigorous atmospheric transport simulations in future work.

The matrix method was a deliberate effort to address criticism raised in the literature (e.g., by Naegler et al., 2007, Battle et al., 2006, and indeed Stephens et al., 1998) that ATM uncertainty reduces the confidence one can place in APO as an evaluation metric for ocean model air-sea fluxes. Some of those papers went so far as to suggest that the uncertainty is so large that APO does not provide a useful constraint. Our matrix method provides a means to quantify the ATM uncertainty, although it likely does tend to exaggerate that uncertainty (the use of the best guess green envelopes and broader gray envelopes was an attempt to show that the most likely range of uncertainty is narrower than the full width of the gray envelopes). Peylin et al, 2013 and other RECCAP papers show *a posteriori* inversion results for CO<sub>2</sub>, so a number of assumptions are needed to cite these papers as evidence that the current generation of ATMs will have converged on

APO relative to the T3L2 models. Further, at least some of the T3L2 are still actively used (e.g., TM3), which makes it a bit awkward to suggest that these ATMs are outdated. In general, we feel some reluctance to undermine our T3L2 matrix approach based on speculative arguments about reduced ATM uncertainty in APO using modern ATMs.

In defense of our matrix method, Transcom3L2 involved a substantial international effort and coordination that, to our knowledge, has not been repeated since. As part of Transcom3 L2, 13 different ATM modeling groups ran simulations with the same surface forcings to generate a large, publicly available database of standard output files, including the pulse-response functions used in our matrix method. The Transcom APO exercise was a spinoff of T3L2 that provides a means for linking and evaluating the T3L2 basis functions to forward simulations of APO with most (9) of the same 13 models. In comparison, the RECCAP effort cited by Reviewer 1 was considerably less standardized and had no obvious connection to APO. It involved “Eleven sets of carbon flux estimates ... generated by different inversions systems that vary in their inversions methods, choice of atmospheric data, transport model and prior information.” While the matrix method used here can be criticized on a number of levels, in the absence of a new, internationally coordinated effort that is beyond the scope and resources of our present work, the pulse-response functions generated by the Transcom modelers provide the most readily available means to compare uncertainty in modeled APO among a wide range of ATMs.

That said, we have added the following sentences to Section 4.2: “In addition, the spread in ATM results has been reduced substantially for CO<sub>2</sub> inversions using post-Transcom3-era ATMs [Peylin *et al.*, 2013], suggesting that ATM uncertainty also may be reduced for forward simulations of APO. If this is the case, then new forward simulations with several different modern-era ATMs may be sufficient to characterize ATM uncertainty, potential reducing it substantially from the broad windows that result from our current matrix approach.” We also have performed some full forward simulations with GEOS-Chem, a modern-era ATM that has been used extensively in CO<sub>2</sub> passive tracer simulations, and obtained results that are generally consistent with our matrix method.



**Review Response supplementary figure 1.** APO at Macquarie Island computed from forward simulations of the GEOS-Chem model forced by 1994-1997 O<sub>2</sub>, N<sub>2</sub> and CO<sub>2</sub> air-sea fluxes from 6 ESM ocean biogeochemistry model components (green curves). Black curves show the observed APO mean annual cycle. The results obtained from these forward simulations with a single ATM are largely consistent with the results obtained from our matrix model method based on the T3L2 pulse response functions. The top row ESMs capture observed APO relatively well, while the bottom row ESMs do not.

2) This study evaluates 6 ocean biogeochemistry models that were part of CMIP5, but there were more participating models and the text does not explain why these 6 were chosen. Is there something special that distinguishes them from others? If this work is intended primarily as a demonstration of a method, then 6 models is sufficient, but this should be explained clearly in the introduction.

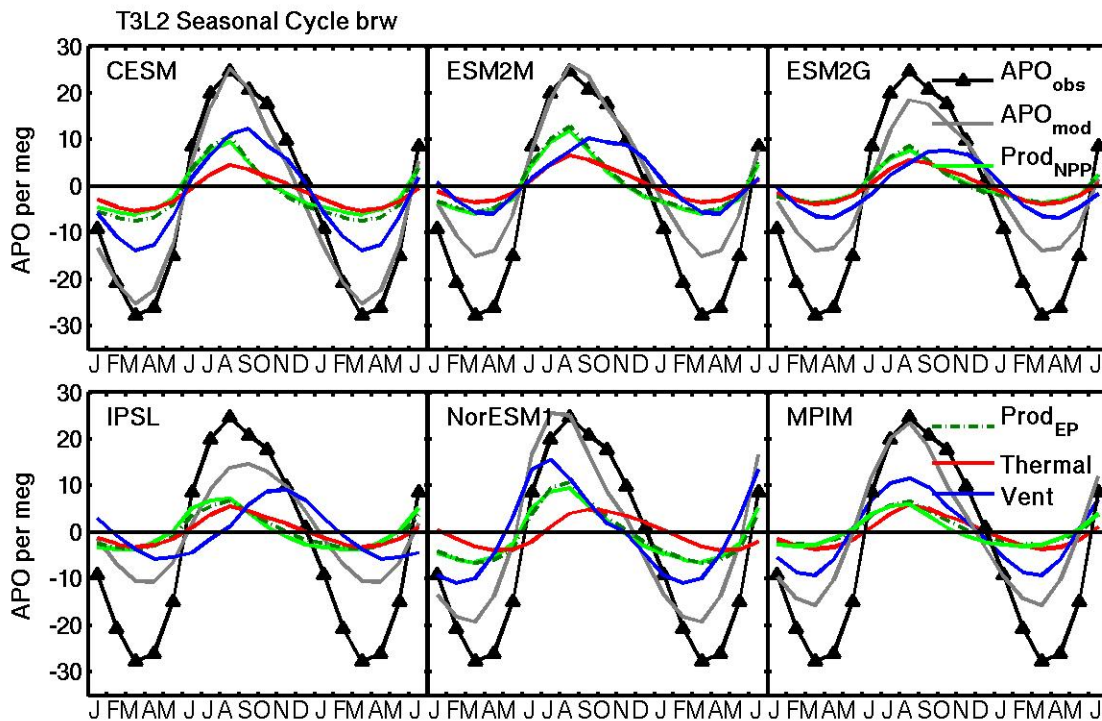
We explain more explicitly in Section 2.1, that, “Many of these (needed CMIP5 output) fields were available through public web interfaces, but some variables, particularly Q, required assistance from the individual modeling groups, which effectively limited the study to 6 models listed above.” We have also stated in the Introduction that, “This work is intended primarily as a demonstration of method using an available subset of the CMIP5 ESMs rather than as a comprehensive evaluation of all the CMIP5 models.”

3) Equation 2 parses FO<sub>2</sub>total as the sum of FO<sub>2</sub>n<sub>cp</sub>, FO<sub>2</sub>v<sub>ent</sub> and FO<sub>2</sub>t<sub>herm</sub>. The authors have confidence in FO<sub>2</sub>t<sub>herm</sub> and 2 methods for estimating FO<sub>2</sub>n<sub>cp</sub>. FO<sub>2</sub>v<sub>ent</sub> is then estimated as a

residual and the authors conclude that in many places it is unreasonable so they do not use it. However, if FO2vent calculated as a residual is wrong, then one of the other terms must also be wrong. Unless the authors can explain how FO2vent as a residual could be wrong while FO2ncp is right, then I don't think FO2ncp should be used individually either. Rather, a combined FO2bio should be calculated as a residual and used.

Partitioning  $APO_{bio}$  into  $APO_{NCP}$  and  $APO_{vent}$  components was an important goal of this paper, because isolating  $APO_{NCP}$  is the most straightforward way to compare APO directly to satellite ocean color data (see discussion in Nevison et al., 2012a). Rather than showing only  $APO_{bio}$ , we think it is more useful to at least attempt the partitioning, and then discuss why it may be falling short in some regions (like the Southern Ocean).

To specifically address the reviewer's comment, we now include the  $APO_{vent}$  term in Figure 3 (now Figure 4) (at Barrow, AK), while including caveats that, “ $APO_{vent}$  can be estimated only as a residual of 3 other terms using standard CMIP5 output and thus its shape and phasing are sensitive to even small uncertainties in those other terms. Thus, the residual ventilation curves in Figure 4 should be interpreted with caution (e.g., the NorESM1 curve is clearly unreasonable in phasing).”



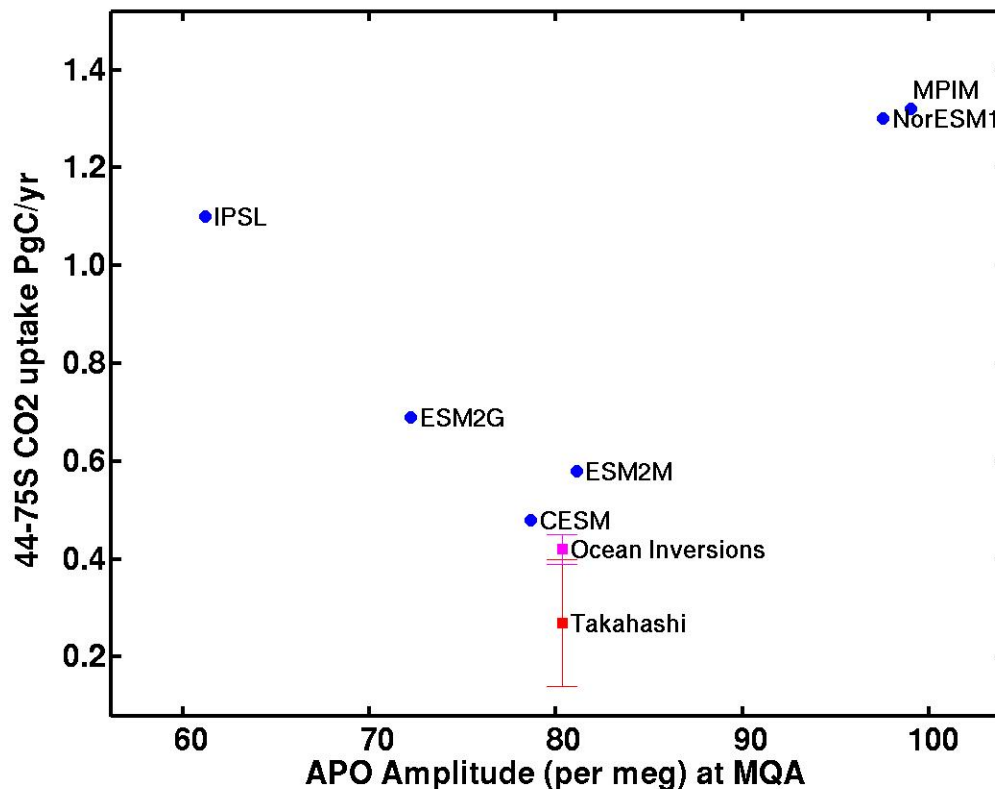
**New Figure 4**, partitioning  $APO_{ncp}$ ,  $APO_{therm}$  and  $APO_{vent}$  at Barrow.

At the end of Methodology Section 2.2.3 we also have added text to clarify the rationale for considering  $APO_{NCP}$  in the Southern Ocean while avoiding  $APO_{vent}$ , “While the problems with  $APO_{vent}$  necessarily imply a corresponding problem in one or both of the

other component terms  $\text{APO}_{\text{NCP}}$  and  $\text{APO}_{\text{therm}}$ , as discussed below, the shape of these latter terms is still informative and is less sensitive to the uncertainties inherent in the residually-estimated  $\text{APO}_{\text{vent}}$  term.”

4) Some discussion of the relevance of the model-assessment results discussed here for assigning confidence to future carbon-climate projections by these models would be valuable. Are the poor-performing models at all distinct in their projections of future  $\text{CO}_2$  uptake by the ocean? Does this method have promise as a tool for evaluating future climate projections?

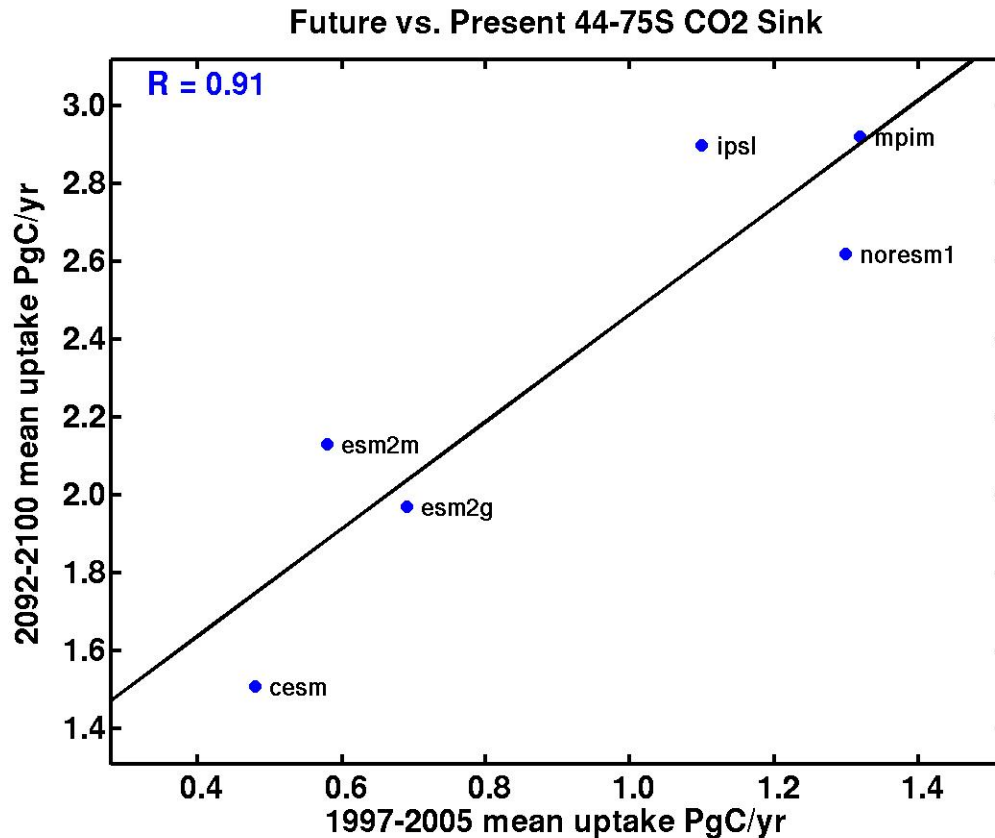
We have included a new Figure 10 that addresses this question, at least with respect to present day ESM prediction of  $\text{CO}_2$  uptake in the Southern Ocean.



The **new Figure 10** shows annual mean  $\text{CO}_2$  uptake in the Southern Ocean for 1997-2005 integrated from 44-75°S and plotted vs. mean APO amplitude at Macquarie over the same period. We discuss in Section 4.2 how the ESMs that reproduce APO the best in the Southern Ocean tend to predict a smaller present day net carbon uptake between 44-75° than those (IPSL, MPIM, NorESM1) that perform more poorly on APO. As shown in Figure 9, the top performing models on APO are also in better agreement with independent estimates of carbon uptake from ocean inversions and observed  $\text{pCO}_2$  databases [Lenton *et al.*, 2013].

Reviewer Stephens also asks about future  $\text{CO}_2$  uptake. Since our current manuscript focuses on the historical (1850-2005) CMIP5 simulations, this question is probably beyond the scope of the present work. However, we note here that our further work with

the RCP8.5 future scenario, based on mean results from 2092-2100 for the same 6 ESMS, suggests that present day and future CO<sub>2</sub> uptake are well correlated. This suggests that the models that perform poorly on CO<sub>2</sub> uptake in the present day may tend to overestimate future Southern Ocean CO<sub>2</sub> uptake.



**Review response supplementary figure 2**, showing annual mean CO<sub>2</sub> uptake in the Southern Ocean for 1997-2005 integrated from 44-75°S compared to annual mean CO<sub>2</sub> uptake from 2092-2100 under the RCP8.5 forcing scenario.

5) If the only information coming from satellite ocean color is phasing, would it not be simpler to just use satellite NPP, which presumably has very similar phasing? Some discussion of the value of satellite NCP estimates in the context of phase information only (if there is one) would be useful.

We have effectively done this by using satellite NPP rather than NCP/EP in Figures 5-8. However, since NCP/EP is in principle more closely related to  $APON_{NCP}$ , we think it is useful to consider both quantities (as in Figure 4). Discussing the relationship between satellite NCP and EP also provides a background for one of the points in our Conclusion, "Improving the understanding of the relationship between model air-sea O<sub>2</sub> fluxes and quantities like NPP, NCP and EP is a more tractable problem that can be dissected with appropriate model diagnostics, e.g., as per *Manizza et al.* [2012]. Extending model-derived insights to satellite products may be more challenging and will likely require a shift in emphasis from EP at an arbitrary reference depth to near-surface

processes like NCP, which are more relevant for exchanges of O<sub>2</sub> and CO<sub>2</sub> at the air-sea interface and more directly related to upward radiances detected by satellites.”

Response to minor comments annotated in the text. We have followed all the reviewer’s suggestions, unless specifically noted. Since many of the suggestions are minor wording changes, we only explicitly respond to the comments that required substantial changes:

p.6 comment 1: We have added, “The first step, estimation of chlorophyll is known to have significant bias (underestimation by ~2-3 times) in the Southern Ocean which is transferred to higher level products. We correct for that by using algorithms tuned to Southern Ocean datasets blended with more or less standard products elsewhere [Mitchell and Kahru, 2009; Kahru and Mitchell, 2010]. While our satellite estimates of EP are improved, they are still subject to high uncertainty.”

p.7 comments 1-3 were addressed by rewriting paragraph 3 of Section 2.1 as follows:  
For each model, the following output fields were obtained for the CMIP5 standard historical simulation\*, which is driven by prescribed atmospheric CO<sub>2</sub> from 1850-2005: carbon export flux at 100 m depth (EP<sub>100</sub>), vertically integrated NPP, net air-sea O<sub>2</sub> and CO<sub>2</sub> fluxes, net surface heat flux (Q), and sea surface salinity and temperature (SST). Many of these fields were available through public web interfaces\*\*, but some variables, particularly Q, required assistance from the individual modeling groups, which effectively limited the study to 6 models listed above.

\*other CMIP5 intercomparisons (e.g., Anav et al., 2013) do not provide explicit references or meteorological drivers for the historical simulation. We have followed this precedent of describing the historical simulation as one that is driven by a standard prescribed atmospheric CO<sub>2</sub> concentration from 1850-2005. As for the meteorological drivers, these are model specific and thus described in the individual references for each model.

\*\* while these web interfaces exist, in practice we received most of the output directly from the modeling groups, and therefore have included representatives from each group as coauthors (except in one case where the modeler preferred to be included in the acknowledgements). This is the main reason the study was limited to six models. We also felt that those models provided a sufficient range of results to illustrate the use of APO as an evaluation metric.

p.8 comment 2 – we have cited Gurney et al., 2003, in which their Fig. 1 provides a map of the 11 ocean regions from Transcom3.

p.8 comment 3 – We have clarified that Transcom 3 uses an annually repeating cycle of meteorology. “...using an annually repeating cycle of meteorology that was model specific for each ATM” Table 1 in the cited Gurney et al. 2003 lists the meteorological drivers for each model.

p.10 comment 1. Clarified that we used, “station output from the forward ATM simulations of the APO Transcom Experiment.”

p.10 comment 2. Inserted, “This evaluation was conducted using a subset of 9 of the original 13 T3L2 ATMs that also participated in APO Transcom. For this subset, the matrix method performed well ...”

p.12 comment 1. Since Section 2.2 is a methodology section, we have tried to avoid presenting results here, but do now cite Table 1, which gives the range of  $ef$  values.

p.12 comment 2. We have decided to show the  $APO_{vent}$  in Figure 4, since omitting it seems to be causing more consternation than simply showing it would. We have also modified the text to explain the rationale for rejecting  $APO_{vent}$  in the Southern Hemisphere while still considering the other component terms (again trying to defer the presentation and discussion of results to later sections), “While the problems with  $APO_{vent}$  necessarily imply a corresponding problem in one or both of the other component terms  $APO_{NCP}$  and  $APO_{therm}$ , as discussed below, the shape of these latter terms is still informative and is less sensitive to the uncertainties inherent in the residually-estimated  $APO_{vent}$  term.”

p.13 comments 1 and 3, replaced with “For the Southern Hemisphere we used an empirical Chl algorithm (SPGANT) that was tuned to in situ Chl in the Southern Ocean and **spatially** blended with the standard SeaWiFS OC4 algorithm [Kahru and Mitchell, 2010]. The same blending scheme was applied when blending NPP between two versions of the **Vertically Generalized Productivity Model** (VGPM) algorithm ...”

p.13 comment 4, we have added,  
“While the Laws [2004] and Dunne *et al.* [2005] methods of deriving EP are not identical, they both estimate export efficiency as a function of sea-surface temperature and NPP, are fitted to *in situ* data, and generally produce similar estimates. In Nevison *et al.* [2012a] the Southern Ocean EP derived with the Laws model was modified by constraining to the bulk nutrient budget estimated in the ocean inversion of Schlitzer [2000]. That reduced the unrealistically high export efficiency of the Laws model observed at cold temperatures and brought it into closer agreement with the Dunne *et al.* export efficiency.”

p.14 comment 1. This sentence is now included “Details of the station locations and time spans of data used to calculate the mean seasonal cycle are listed in Table S2. For MQA (1997-2007) and BRW (1993-2008), the time spans overlapped mostly but not perfectly with the CMIP5 model output (1994-2005) and the satellite data (1997-2009 for SPGANT, 2002-2011 for VGPM).”

p.14 comment 6. We include the following text, “The uncertainty in the observed mean seasonal cycles over the timespan of available data is less than 6% at extratropical latitudes, reflecting a combination of instrumental precision, synoptic variability and interannual variability (IAV) in the seasonal cycle. We reiterate that the current study is focused on the mean seasonal cycle in APO as a first order challenge for the CMIP5 ocean models. Here, model, APO and satellite seasonal cycles are evaluated over roughly comparable periods that are dictated by data availability. The examination of interannual variability is deferred to future research, which will require ATM simulations of APO driven by interannually varying meteorology.”

p.15 comment 1. The reviewer is probably right and we have deleted this sentence. The proposed alternative method for quantifying uncertainty involves an analysis of IAV, which, as stated above, is beyond the scope of the current study.

p.17 comment 2 (see also response to p.12 c1) We have replaced the highlighted text with, “By inference, the missing  $\text{APO}_{\text{vent}}$  term accounts for the difference. However, as discussed in Section 2.2.3,  $\text{APO}_{\text{vent}}$  can be estimated only as a residual of 3 other terms using standard CMIP5 output and thus its shape and phasing are sensitive to even small uncertainties in those other terms. Thus, the residual ventilation curves in Figure 3 should be interpreted with caution (e.g., the NorESM1 curve is clearly unreasonable in phasing).”

p.18 comment 1. We have added this introductory statement, “In the previous sections we considered APO and satellite data as separate evaluation metrics for ESMs. Below we consider the two as combined metrics. While this analysis is limited by uncertainties in the absolute magnitude of satellite NPP and EP/NCP and our imperfect ability to partition the ESM total APO signal into its NCP and other components, it nevertheless provides some additional insight into the behavior of the ESMs.”

p.20 comment 2. We have added, “The inference from the APO component analysis in Figure 3 that the GFDL models may have weak ventilation in the North Atlantic ...”

p.22 comments 1-5. We have rewritten as, “we currently are not able to distinguish which of the underlying air-sea  $\text{O}_2$  flux fields is the most accurate, due to the uncertainty associated with translating these fluxes into an atmospheric signal **using TransCom3 era model responses to uniformly distributed regional fluxes**. However, **even with our current matrix method**, the APO constraint is sufficiently robust to indicate that NorESM1 and MPIM substantially overestimate some combination of production and deep ventilation in the Southern Ocean, while IPSL probably tends to underestimate these fluxes (Table 1, Figure 7a). Reducing ATM uncertainty is a challenging problem that potentially can be addressed by using column-integrated APO signals **from aircraft data [Wofsy et al., 2011]**, or conversely, by using vertical profiles to identify top-performing ATMs [Stephens et al., 2007]. **In addition, the spread in ATM results has been reduced substantially for  $\text{CO}_2$  inversions using post-Transcom3-era ATMs [Peylin et al., 2013], suggesting that ATM uncertainty also may be reduced for forward simulations of APO. If this is the case, then new forward simulations with several different modern-era ATMs may be sufficient to characterize ATM uncertainty, potential reducing it substantially from the broad windows that result from our current matrix approach.**”

p.22 comment 6. We have added, “For example, the Southern Ocean ef-ratios for MPIM and IPSL in that earlier study were about 0.2 and 0.4, respectively, compared to 0.14 and 0.27, respectively, in the current study.”

p.24 comment 1. We have added, “The first of these, ATM uncertainty, is large, as quantified using our Transcom3-based matrix method, but probably also has been overstated in previous analyses [e.g., Naegler et al., 2007]. ATM uncertainty also may

be reduced substantially in future work with modern ATMs and O<sub>2</sub>-specific flux patterns.”

p.33 comments 3 and 6. “The amplitudes are scaled for each ATM and monitoring site based on the validation exercise described in Section 2.2.2 and illustrated in the Supplementary Material. The gray window shows the full range of responses from all 13 T3L2 ATMs, uncorrected based on the Transcom APO validation exercise. The heavy black line shows the observed APO mean annual cycle. a) Results at South Pole, compared to SIO observations.”

p.40 comment 2. We have removed the illegible labels from the tops of each panel in Figure 4.

p.41 comment 1. We have added this to the Fig 5 caption, “The satellite data are from SPGANT/Laws in panel (a) and VGPM/Dunne in panels (b-c).”

p.42 comment 3. We have moved the labels to the top of the panels and enlarged the font.

p.45 comment 1. We have deleted the sea ice figure and replaced it with a new Figure 9 that addresses major comment 5 – relating ESM performance on APO to carbon uptake in the Southern Ocean.

Supplementary Material.

Page 2, comment 1. We have provided more information about the APO Transcom forward simulations (FS):

“In contrast to the matrix-based PRC simulations, which used uniform regional distributions of O<sub>2</sub> and N<sub>2</sub>, the archived APO Transcom forward simulations were forced by fine-scale (0.5 x 0.5 degree) monthly mean air-sea flux distributions (interpolated by APO Transcom from the original 1.125 degree resolution of *Garcia and Keeling* [2001]). The simulations were run by each participating model group with the fluxes turned on for the first year and turned off for the last two years. The resulting ATM atmospheric O<sub>2</sub> and N<sub>2</sub> fields in ppm were sampled in each of the 36 months of the simulations at 253 monitoring sites. The steady-state response, i.e., the mean seasonal cycle, was computed by summing all Januaries, Februaries, etc., for the three years. Conceptually, this calculation assumes that the ATM behaves linearly and that the steady-state response can be represented as the sum of the response to the fluxes from the present year, the past year, and two years previously, which correspond to the first, second, and third years of the simulations, respectively.

In using the archived APO Transcom results, it was necessary to account for several irregularities. First, the JMA O<sub>2</sub> and N<sub>2</sub> results were multiplied by 10<sup>6</sup> to convert to ppm units. Second, TM3 ran all 36 months with pulses on, so instead of summing all 3 sets of Januaries, Februaries, etc., the mean annual cycle was calculated based on the third year of the simulation alone. Finally, GISS UCI in principle was a 10<sup>th</sup> model that participated in both T3L2 and APO Transcom, but in practice it could not be used because only the first (pulse-on) year of GISS UCI output was submitted to APO Transcom.”

Page 2, comment 2. We speculate as to why the sigma ratios might be  $< 1$  at the bottom of Table S2: “At most extratropical stations, the  $\sigma_{\text{pre}}/\sigma_{\text{fs}}$  ratios are  $< 1$ , suggesting that the Pulse Response Code tends to underestimate the true APO amplitude from the forward simulations. This may be due to the uniform flux distributions assumed across Transcom regions, which could smooth out hotspots for  $\text{O}_2$  air-sea flux that may lead to more intense peaks in true APO.”

Page 2, comment 5. We have provided correlation coefficients as  $R^2$ .

Page 3, comment 1. Columns added for time period used for 5 stations in Fig. 1

Page 3, comment 3. We have added the missing 3 stations (RYO, CGO5500m, and MLO) to Table S2.

Page 3, comment 4. We have provided correlation coefficients as  $R^2$ .

Page 5, comments 1,6. We have added the missing 3 stations (RYO, CGO5500m, and MLO) to the Taylor diagrams and provided the Taylor, 2001 reference

## Response to Reviewer 2.

We thank Reviewer 2 for his/her helpful comments, which are reprinted here in blue. Please see our responses in black.

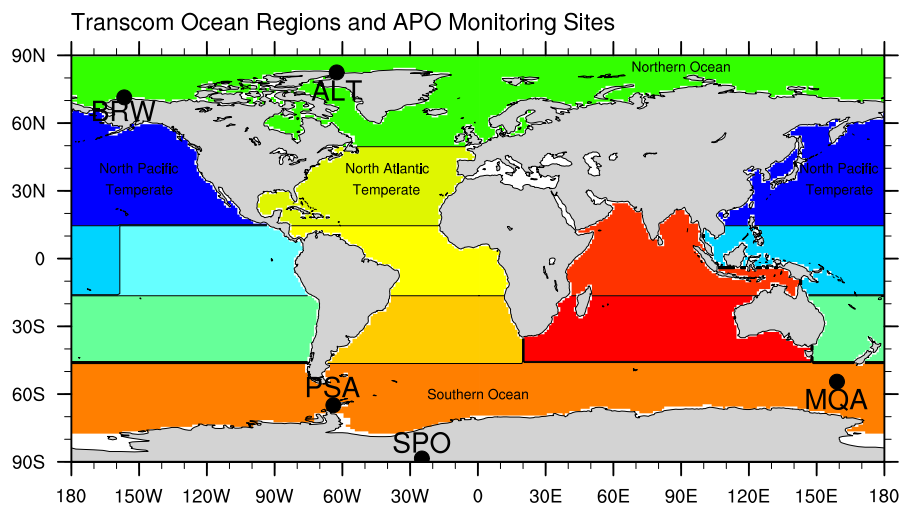
The authors present a comprehensive evaluation of the ocean biogeochemical components of 6 CMIP5 models against observed APO and Satellite estimates of phytoplankton productivity. The goal here is to offer the APO datasets, in particular, as a new constraint on the models. The authors use a transport matrix method so as to speed the process of atmospheric transport substantially. They compare this method to a direct method and only consider regions where this works well. Atmospheric transport uncertainty is smaller than variance across the ocean biogeochemical models for the high latitude sites. This is important, since the utility of APO has generally been questioned by the fact that one must do this transport calculation. The authors could point this out more clearly, i.e. in conclusions. On the whole, this is a nice analysis that should be published after minor revisions.

Major comments: 1. The transport matrix is a good step, and I support its use for this paper. Going forward, the authors might consider developing such a matrix approach based on regions different from the square boxes of TRANSCOM that do not capture the biogeography of the ocean well. Fay and McKinley (2014) offer global biomes that would be preferable. For this paper, the authors need to clarify if the aggregation across these square biomes could impact their results and the model-to-model differences that are found. Specifically, if models don't have their major biogeochemical gradients across the TRANSCOM region boundaries, could this influence these comparisons? I also ask that TRANSCOM region boundaries be included in at least one panel in Figure 4. Fay, A. R. & McKinley, G. A. Global open-ocean biomes: mean and temporal variability. *Earth Syst. Sci. Data* 6, 273–284 (2014).

The matrix method was a deliberate effort to address criticism raised in the literature (e.g., by Naegler et al., 2007, Battle et al., 2006, Stephens et al., 1998) that ATM uncertainty reduces the confidence in APO as an evaluation metric for ocean model air-sea fluxes. Some of those papers went so far as to suggest that the uncertainty is so large that APO does not provide a useful constraint. The matrix method provides a means to quantify the ATM uncertainty. Somewhat surprisingly, our first reviewer suggested that ATM uncertainty is no longer as important a problem and therefore it would be better to use full forward simulations than the matrix method. While we concede that he may be right, we are also concerned that he may be dismissing too casually the lingering issues with ATM uncertainty, especially since he does not offer direct proof that ATM uncertainty is no longer a major problem for APO analyses. Please see our response to Reviewer 1 for further discussion.

We agree with Reviewer 2 that the latitude-based boundaries of Transcom3, which we now show in our new Figure 1, are not ideal for capturing the main biogeochemical boundaries. The biomes defined in Fay and McKinley, 2014 would likely be an improvement, and the partitioning of the Southern Ocean into 3 different regions based on biogeochemical function, could provide insight into the contribution of these different regions to variability in APO. While it is beyond the scope and resources of the present study to rerun the T3L2 basis functions to create new biome-oriented basis functions, we now discuss the advantages of this strategy in the following text added to the Discussion,

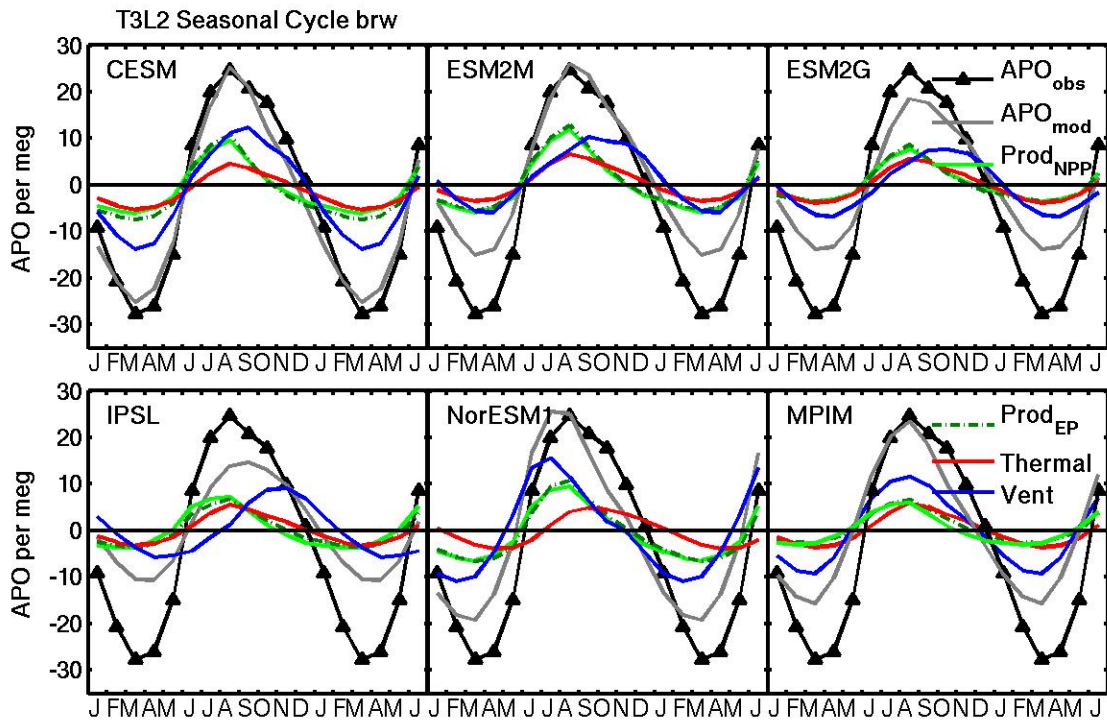
“In addition, the spread in ATM results has been reduced substantially for CO<sub>2</sub> inversions using post-Transcom3-era ATMs [Peylin *et al.*, 2013], suggesting that ATM uncertainty also may be reduced for forward simulations of APO. If this is the case, then new forward simulations with several different modern-era ATMs may be sufficient to characterize ATM uncertainty. Alternatively, it may be valuable to continue with a matrix-based approach, using basis functions from many ATMs, but with redefined regional boundaries that are not defined based simply on latitude, as in T3L2 (Figure 1), but rather that correspond to the biogeography of major ocean regions [Fay and McKinley, 2014]. The definition of such basis functions could help extend the utility of the matrix approach to lower latitude APO monitoring sites and allow for the partitioning of the Southern Ocean into multiple regions defined around biogeochemical function, while still retaining the advantages of the matrix method, i.e., the ability to quickly and easily compare multiple ATMs forced with the same air-sea fluxes.”



**New Figure 1**

2. It is unfortunate that the Ventilation and NCP signals cannot be distinguished; and at the same time the NCP estimates from satellite are so uncertain that we have a reasonably loose constraint here. Showing the APO<sub>vent</sub> estimated as a residual would be helpful in Figure 3 to add to the text discussion and to better highlight this issue.

We now include the APO<sub>vent</sub> term in Figure 4 (at Barrow, AK), while including caveats that, “APO<sub>vent</sub> can be estimated only as a residual of 3 other terms using standard CMIP5 output and thus its shape and phasing are sensitive to even small uncertainties in those other terms. Thus, the residual ventilation curves in Figure 4 should be interpreted with caution (e.g., the NorESM1 curve is clearly unreasonable in phasing).”



**New Figure 4** (formerly 3), partitioning  $APON_{cp}$ ,  $APOtherm$  and  $APOVent$  at Barrow.

At the end of Methodology Section 2.2.3 we also have added text to clarify the rationale for considering  $APON_{CP}$  in the Southern Ocean while avoiding  $APOVent$ , “While the problems with  $APOVent$  necessarily imply a corresponding problem in one or both of the other component terms  $APON_{CP}$  and  $APOtherm$ , as discussed below, the shape of these latter terms is still informative and is less sensitive to the uncertainties inherent in the residually-estimated  $APOVent$  term.”

3. The conclusions state that the major issues are ATM uncertainty and uncertainty in EP100. The paper suggests to me that the ventilation separation is also quite important, and that the ATM transport is a smaller issue at the high latitudes where this paper focuses. The ATM transport issue at lower latitudes may be more an issue of the TRANSCOM region definitions and how to turn a forward model into a matrix transport approach – but this is really more a technical issue with respect to the challenge of running atmospheric models than about uncertainty in ATM transport. Overall in the conclusions, the authors need to clarify better the many issues that they reveal with their analysis so as to leave the reader with a clearer picture of the value of APO in ESM evaluation, and the remaining challenges to increasing its utility. This discussion might be well-served by a clear separation between Northern high latitudes, mid/low latitudes, and Southern high latitudes.

We have revised the Conclusions as follows to address these points:

“At least two primary uncertainties limit our ability to place stronger constraints on ocean model biogeochemistry based on currently available information from APO and satellite data: 1) The relatively large ATM uncertainty involved in translating air-sea  $O_2$  fluxes into APO signals. 2) The uncertainty in how model  $EP_{100}$  relates to the true model  $F_{O_2,NCP}$  flux and how this relationship varies across models and satellite algorithms. The first of these, ATM uncertainty, is large, as quantified using our Transcom3-based matrix method. However, it probably has been overstated in previous analyses, which in some cases went so far as to suggest that APO does not provide a useful constraint on ocean model fluxes [e.g., Naegler *et al.*, 2007]. Further, ATM uncertainty could be reduced substantially in future work with modern ATMs and  $O_2$ -specific flux patterns, or with new regional boundaries defined based on ocean biogeography rather than simple latitude. Even within the limits of our current approach, we have shown that half of the 6 ESMs tested here produce APO cycles whose mismatch with observed APO clearly transcends ATM uncertainty, suggesting underlying deficiencies in those models’ physics and biogeochemistry.

Improving the understanding of the relationship between model air-sea  $O_2$  fluxes and quantities like NPP, NCP and EP is a more tractable problem that can be dissected with appropriate model diagnostics, e.g., as per Manizza *et al.* [2012]. In the current analysis, using standard CMIP5 output from 6 ocean biogeochemistry models, we encountered difficulties in relating  $F_{O_2}$  to EP and NCP, which hindered our ability to diagnose the mechanisms responsible for model performance and to compare ESM-derived  $APO_{NCP}$  directly to satellite-based  $APO_{NCP}$  signals. Extending model-derived insights to satellite products likely will require a shift in emphasis from EP at an arbitrary reference depth to near-surface processes like NCP, which are more relevant for exchanges of  $O_2$  and  $CO_2$  at the air-sea interface and more directly related to upward radiances detected by satellites.”

Response to minor comments annotated in the text.

p.8488: We have replaced with, “The exported carbon subsequently is respired in the subsurface ocean, leading to  $O_2$  depletion at depth.  $O_2$  is replenished by...”.

p.8488 comment 2: We have expanded to, “both closely linked to the biological pump critical that draws carbon out of surface waters and is critical for ocean uptake of atmospheric  $CO_2$ ...”

p.8489 : We have cited, “Many biogeochemical processes that are expected to occur in the future, such as responses to warming and stratification, are also highly relevant on seasonal time scales [Keeling *et al.*, 2010; Anav *et al.*, 2013].” (Both citations are already in the References.)

p. 8492. We have added, “In this equation,  $Q$  is heat flux,  $(dS/dT)_{N_2}$  is the temperature derivative of the  $N_2$  solubility coefficient, and  $C_p$  is the heat capacity of sea water.”

p. 8496. We now show the  $APO_{vent}$  term in Figure 4 (formerly 3) and have replaced the highlighted text with, “We therefore do not attempt to explicitly resolve or present

APO<sub>vent</sub> signals in the Southern Hemisphere. While the problems with APO<sub>vent</sub> necessarily imply a corresponding problem in one or both of the other component terms APO<sub>NCP</sub> and APO<sub>therm</sub>, as discussed below, the shape of these latter terms is still informative and is less sensitive to the uncertainties inherent in the residually-estimated APO<sub>vent</sub> term.”

p. 8497, In response to this and another query from Reviewer 1, we have added, “While the *Laws* [2004] and *Dunne et al.* [2005] methods of deriving EP are not identical, they both estimate export efficiency as a function of sea-surface temperature and NPP, are fitted to *in situ* data, and generally produce similar estimates.” We have also clarified that NPP was downloaded from <http://science.oregonstate.edu/ocean.productivity>.

p. 8501, APO<sub>vent</sub> is now shown in Figure 3.

p. 8504, Have replaced this sentence with, “The inference from the APO component analysis in Figure 3 that the GFDL models may have weak ventilation in the North Atlantic appears to contradict the analysis of *Dunne et al.* [2012], who found robust NADW formation in both the ESM2M and ESM2G versions, but possibly could be reconciled if the biogeochemical gradients across which deep water formation acts are too weak.”

p. 8527 Figure 7 Y-labels are both now “Amplitude per meg”.

p. 8517 we have added a new Figure 1 showing both the Transcom regions and the locations of APO stations featured in Figure 2 (see above).

1    **Evaluating the ocean biogeochemical components of earth system models**  
2    **using atmospheric potential oxygen (APO) and ocean color data**

3

4    C.D. Nevison<sup>1</sup>, M. Manizza<sup>2</sup>, R.F. Keeling<sup>2</sup>, M. Kahru<sup>2</sup>, L. Bopp<sup>3</sup>, J. Dunne<sup>4</sup>, J. Tiputra<sup>5</sup>, T.

5    Ilyina<sup>6</sup>, B.G. Mitchell<sup>2</sup>

6    <sup>1</sup> University of Colorado, Boulder, Institute for Arctic and Alpine Research, Boulder, Colorado

7    <sup>2</sup> Scripps Institution of Oceanography, La Jolla, California.

8    <sup>3</sup> IPSL/LSCE, UMR8212, CNRS-CEA-UVSQ, Gif sur Yvette, France

9    <sup>4</sup> National Oceanic and Atmospheric Administration/Geophysical Fluid Dynamics Laboratory,

10    Princeton, New Jersey

11    <sup>5</sup> Uni Climate, Uni Research and Bjerknes Centre for Climate Research, Bergen, Norway.

12    <sup>6</sup> Max Planck Institute for Meteorology, Hamburg, Germany.

13

14

Cynthia Nevison 10/20/2014 2:11 PM

**Formatted:** Superscript

Cynthia Nevison 10/20/2014 2:12 PM

**Deleted:** Allegaten 70, 5007

Cynthia Nevison 10/20/2014 2:14 PM

**Formatted:** Font:(Default) Times New Roman, 12 pt

Cynthia Nevison 10/20/2014 2:14 PM

**Formatted:** Font:(Default) Times New Roman, 12 pt

1   **Abstract**

2   The observed seasonal cycles in atmospheric potential oxygen (APO) at a range of mid to high  
3   latitude surface monitoring sites are compared to those inferred from the output of 6 Earth  
4   System Models participating in the fifth phase of the Coupled Model Intercomparison Project  
5   (CMIP5). The simulated air-sea O<sub>2</sub> fluxes are translated into APO seasonal cycles using a matrix  
6   method that takes into account atmospheric transport model (ATM) uncertainty among 13  
7   different ATMs. Three of the ocean biogeochemistry models tested are able to reproduce the  
8   observed APO cycles at most sites, to within the large TransCom3-era ATM uncertainty used  
9   here, while the other three generally are not. Net Primary Production (NPP) and net community  
10   production (NCP), as estimated from satellite ocean color data, provide additional constraints,  
11   albeit more with respect to the seasonal phasing of ocean model productivity than overall  
12   magnitude. The present analysis suggests that, of the tested ocean biogeochemistry models,  
13   CESM and GFDL ESM2M are best able to capture the observed APO seasonal cycle at both  
14   Northern and Southern Hemisphere sites. Uncertainties in most models can be attributed to the  
15   underestimation of NPP, deep ventilation or both in the northern oceans.

16

17   **Introduction**

18   Ocean physical and biogeochemical processes have profound influences on Earth's climate.  
19   Phytoplankton in the sunlit part of the ocean convert carbon from inorganic to organic form via  
20   photosynthesis, thereby establishing the base of the ocean food chain. Primary production and  
21   subsequent export of organic carbon from the mixed layer (export production) and  
22   remineralization at depth are key components of the so called "biological pump," which

Cynthia Nevison 10/20/2014 2:19 PM

Deleted: Half

Cynthia Nevison 10/20/2014 2:19 PM

Deleted: current

Cynthia Nevison 10/20/2014 2:20 PM

Deleted: half

Cynthia Nevison 10/27/2014 11:13 AM

Deleted: or

1 regulates the partition of carbon between the ocean and atmosphere [Gruber and Sarmiento,  
2 2002; Boyd & Doney, 2003].

3 Net community production (NCP) and the related process of export production (EP) are also  
4 important for understanding the distribution of dissolved O<sub>2</sub> within the ocean and the flux of O<sub>2</sub>  
5 (F<sub>O2</sub>) at the air-sea interface. NCP is defined here as the net amount of organic carbon fixed  
6 through photosynthesis over the depth of the mixed layer after accounting for grazing and both  
7 autotrophic and heterotrophic respiration. NCP is closely linked to F<sub>O2</sub>, since each mole of  
8 photosynthetically-fixed carbon that persists beyond the time scale of air-sea exchange (2-3  
9 weeks) leaves a stoichiometric amount of O<sub>2</sub> available for release to the atmosphere. This  
10 release of O<sub>2</sub> to the atmosphere in association with NCP occurs mainly in the spring and summer  
11 at extratropical latitudes [Keeling et al., 1993]. EP more or less balances NCP when averaged  
12 over a full year or if the upper ocean is in a long-term steady state and advective fluxes are zero  
13 [Laws et al., 2000]. The exported carbon subsequently is respired in the subsurface ocean,  
14 leading to O<sub>2</sub> depletion at depth. O<sub>2</sub> is replenished by absorption from the atmosphere when the  
15 deep waters mix back to the surface in fall and winter. Deep ventilation and NCP thus are  
16 distinct processes that are largely separate in time and space but are both closely linked to the  
17 biological pump critical that draws carbon out of surface waters and is critical for ocean uptake  
18 of atmospheric CO<sub>2</sub>.

19 To explore the impacts of future climate change on Earth's climate and ecosystems, the Coupled  
20 Model Intercomparison Project phase 5 (CMIP5) relies on 3-dimensional numerical Earth  
21 System Models (ESMs), which incorporate descriptions of biogeochemical impacts of land and  
22 marine biota. Projections of future atmospheric CO<sub>2</sub> levels and associated climate warming in  
23 CMIP5 depend not only on fossil fuel use projections but also on assumptions about uptake and

Cynthia Nevison 10/27/2014 11:14 AM

**Deleted:** E

Cynthia Nevison 10/27/2014 11:15 AM

**Deleted:** and the related process of net community production (NCP)

Cynthia Nevison 10/20/2014 2:23 PM

**Deleted:** [Keeling et al., 1993]

Cynthia Nevison 10/20/2014 2:23 PM

**Deleted:** R

Cynthia Nevison 10/20/2014 2:23 PM

**Deleted:** [Manizza et al., 2012]

Cynthia Nevison 10/27/2014 11:16 AM

**Deleted:** , which

Cynthia Nevison 10/20/2014 2:25 PM

**Deleted:** both NCP in spring and summer and

1 storage of carbon by the land and ocean. The oceans have absorbed approximately one third of  
2 the anthropogenic carbon released to the atmosphere since the beginning of the industrial era  
3 [*Khatiwala et al.*, 2009], but this fractional rate of uptake is unlikely to continue in the future as  
4 the buffering capacity of surface waters declines and the export of carbon from the surface to the  
5 deep ocean fails to keep pace with anthropogenic fossil fuel combustion [*Arora et al.*, 2013].  
6 Changes in ventilation of abyssal deepwater are an additional possible consequence of future  
7 climate forcing that current models may or may not be able to predict accurately [*Sigman et al.*,  
8 2010].

9 Recent studies have tested the present-day skill of the ocean components of ESMs and some  
10 have also examined future projections [*Schneider et al.*, 2008; *Steinacher et al.*, 2010, *Bopp et al.*  
11 2013; *Anav et al.*, 2013]. These evaluations have compared model output to both hydrographic  
12 measurements and remotely sensed ocean color products, most commonly net primary  
13 production (NPP). The models predict spatial-annual patterns in NPP that reproduce some of the  
14 main features seen in satellite data, but differ over a factor of 2 in NPP magnitude. Some  
15 evaluations have examined seasonal variability and have found that ocean models tend to  
16 underestimate observed NPP at high latitudes (poleward of 44°) in the Northern Hemisphere and  
17 overestimate it in the Southern Hemisphere. The models also fail to capture the timing of the  
18 observed high latitude peak in NPP in both hemispheres, with predictions that are often 1-2  
19 months earlier than observations [*Anav et al.*, 2013; *Henson et al.*, 2013]. However, ocean  
20 color-derived NPP values are uncertain, especially in the Southern Ocean, reducing confidence  
21 in the “observed” constraints.

22 Many biogeochemical processes that are expected to occur in the future, such as responses to  
23 warming and stratification, are also highly relevant on seasonal time scales [*Keeling et al.*, 2010;

1 [Anav et al., 2013](#)]. Thus, challenging models against known seasonal variations can aid in the  
2 development of credible predictions of future changes. Here, we evaluate 6 earth system models  
3 used in CMIP5 against two cross-cutting metrics, which test the models' ability to account for  
4 changes in ocean biogeochemistry on seasonal time frames. [This work is intended primarily as a](#)  
5 [demonstration of method using an available subset of the CMIP5 ESMs rather than as a](#)  
6 [comprehensive evaluation of all the CMIP5 models](#). The first metric is based on satellite-derived  
7 estimates of ocean color, focusing on NPP and NCP. The second metric is based on the seasonal  
8 cycles in atmospheric potential oxygen (APO), an atmospheric tracer that varies seasonally  
9 mainly due to air-sea exchanges of O<sub>2</sub> [*Stephens et al.*, 1998; *Manning and Keeling*, 2006].

10 [NCP](#) is the ocean color-derived flux most relevant to the biological pump, but cannot be directly  
11 observed by remote sensing. It is derived by a combination of remote measurements and poorly  
12 constrained models, which inherently increases its uncertainty [*Schneider et al.*, 2008; *Nevison et*  
13 *al.*, 2012a]. The quantity actually observed from space is spectral top of the atmosphere  
14 radiance, which is used to estimate chlorophyll (or another proxy of phytoplankton biomass);  
15 chlorophyll and other variables such as photosynthetic radiation are used to estimate NPP and  
16 finally, NPP is used to estimate EP. [The first step, estimation of chlorophyll, is known to have](#)  
17 [significant bias \(underestimation by ~2-3 times\) in the Southern Ocean which is transferred to](#)  
18 [higher level products. We correct for that bias by using algorithms tuned to Southern Ocean](#)  
19 [datasets blended with more or less standard products elsewhere](#) [*Mitchell and Kahru*, 2009; *Kahru*  
20 *and Mitchell*, 2010]. [While our satellite estimates of EP are improved, they are still subject to high](#)  
21 [uncertainty.](#)▼

22 Observed seasonal cycles in APO provide a new benchmark for the ocean biogeochemistry  
23 model components of ESMs. They offer evaluation metrics complementary to ocean color

Cynthia Nevison 10/24/2014 11:28 AM

Deleted: available

Cynthia Nevison 10/20/2014 2:30 PM

Deleted: E

Cynthia Nevison 10/21/2014 3:06 PM

Deleted: We address the commonly observed bias in standard satellite algorithms by using algorithms tuned to Southern Ocean datasets [*Mitchell and Kahru*, 2009] blended with more or less standard products elsewhere [*Kahru and Mitchell*, 2010].

1 products by providing additional information on deep ventilation processes unavailable from  
2 satellite data alone. The main drawback of APO seasonal cycles is that atmospheric transport  
3 models (ATMs) are needed to translate ocean model air-sea O<sub>2</sub> fluxes into a seasonal APO  
4 signal, which inevitably introduces uncertainty [Stephens *et al.*, 1998; Nevison *et al.*, 2012a]. A  
5 first attempt has been made to use APO seasonal cycles to evaluate ocean-only marine  
6 biogeochemistry models [Naegler *et al.*, 2007], but the models in that study implemented a  
7 simplified parameterization of the biological processes affecting O<sub>2</sub> and CO<sub>2</sub> air-sea fluxes and  
8 were considerably less advanced than the current ecosystem dynamics and biogeochemical  
9 components used in state-of-the-art ESMs. Further, while Naegler *et al.* asserted that the  
10 uncertainty introduced by ATMs was too large to provide a strong constraint on ocean model  
11 fluxes, their study relied on only two ATMs. Here, we translate the model air-sea fluxes into  
12 APO signals using a wider range of ATMs and show that, in many cases, the discrepancies  
13 between modeled and observed APO seasonal cycles transcend ATM uncertainty.

## 14 **2. Methods**

### 15 **2.1 Ocean Biogeochemistry Models**

16 The CMIP5 models analyzed in this study include the Geophysical Fluid Dynamics Laboratory  
17 (GFDL) Earth System Models (depth-based ESM2M and density-based ESM2G vertical oceans;  
18 Dunne *et al.*, 2012) from Princeton, New Jersey; the Institut Pierre-Simon Laplace Coupled  
19 Model 5 in its low resolution version (IPSL-CM5A-LR, referred to as IPSL in the following)  
20 model from Paris, France; the Community Ecosystem Model (CESM) from the National Center  
21 for Atmospheric Research in Boulder, CO, the Max Planck Institut fuer Meteorologie (MPIM)  
22 Earth System Model, version MPI-ESM-LR, from Hamburg, Germany; and the Norwegian Earth

1 System Model (NorESM1-ME, referred here as NorESM1). The ocean biogeochemical models  
2 embedded in the respective ESMs are represented by TOPAZ (GFDL) [Dunne *et al.*, 2013],  
3 PISCES (IPSL) [Aumont and Bopp 2006], BEC (CESM) [Moore *et al.*, 2002, 2004, 2013], and  
4 HAMOCC (MPIM) [Ilyna *et al.*, 2013]. NorESM1 uses a variant of HAMOCC, adapted to a  
5 sigma coordinate ocean circulation model [Tjiputra *et al.*, 2013].

6 The six ESMs differ in their physical components and implement ocean biogeochemical schemes  
7 that vary in their specifics, but have many common features. All include explicit representations  
8 of upper ecosystem dynamics that distinguish at least one phytoplankton group and one size class  
9 of zooplankton. Four of the models (CESM, both GFDL variants and IPSL) divide  
10 phytoplankton further into at least 2 size classes: large (micro) and small (nano + pico). GFDL  
11 and CESM also explicitly model diazotrophs. Phytoplankton growth rates in all models are co-  
12 limited by light, temperature and nutrient (N, P, Si, Fe) availability. Carbon export flux is closely  
13 linked to ecosystem structure and dynamics, with higher sinking rates assumed for large  
14 phytoplankton, representing, e.g., diatoms.

15 For each model, the following output fields were obtained for the CMIP5 standard historical  
16 simulation, which is driven by prescribed atmospheric CO<sub>2</sub> from 1850-2005: carbon export flux  
17 at 100 m depth (EP<sub>100</sub>), vertically integrated NPP, net air-sea O<sub>2</sub> and CO<sub>2</sub> fluxes, net surface heat  
18 flux (Q), and sea surface salinity and temperature (SST). Many of these fields were available  
19 through public web interfaces, but some variables, particularly Q, required assistance from the  
20 individual modeling groups, which effectively limited the study to 6 models listed above. The  
21 EP<sub>100</sub> and NPP fields were compared directly to the corresponding satellite ocean color products.  
22 The remaining 5 output fields were used in the estimation of APO time series, with the final  
23 three fields used to estimate air-sea N<sub>2</sub> fluxes based on the  $Q(dS/dT)_{N_2}/C_p$  equation [Keeling *et*

Cynthia Nevison 10/20/2014 2:47 PM

**Deleted:** O

Cynthia Nevison 10/20/2014 2:46 PM

**Deleted:** was

Cynthia Nevison 10/20/2014 2:47 PM

**Deleted:** from the six models

Cynthia Nevison 10/21/2014 10:39 AM

**Deleted:** (1850-2005)

Cynthia Nevison 10/21/2014 10:39 AM

**Deleted:** case

Cynthia Nevison 10/20/2014 2:44 PM

**Deleted:** either directly from the individual modeling groups or through a collective web interface created for the CMIP5. The output fields included carbon export flux at 100 m depth (EP<sub>100</sub>), vertically integrated NPP, net air-sea O<sub>2</sub> and CO<sub>2</sub> fluxes, net surface heat flux (Q), and sea surface salinity and temperature (SST).

Cynthia Nevison 10/21/2014 10:41 AM

**Deleted:** first two

Cynthia Nevison 10/21/2014 10:41 AM

**Formatted:** Subscript

1 | *al.*, 1993; *Manizza et al.*, 2012] with modifications from *Jin et al.* [2007]. In this equation,  $Q$  is  
2 | heat flux,  $(dS/dT)_{N_2}$  is the temperature derivative of the  $N_2$  solubility coefficient, and  $C_p$  is the  
3 | heat capacity of sea water. The resulting  $N_2$  fluxes, together with the prognostic  $O_2$  and  $CO_2$  air-  
4 | sea fluxes, were used as described below to force atmospheric transport model simulations to  
5 | compute atmospheric time series of APO [*Naegler et al.*, 2007; *Nevison et al.*, 2008; 2012a].  
6 | Since all the ocean models operated on an irregular, off-polar grid with 2-dimensional latitude  
7 | and longitude coordinates, these were first interpolated to a regular  $1^\circ \times 1^\circ$  latitude/longitude grid  
8 | using Climate Data Operators freeware (<https://code.zmaw.de/projects/cdo>). The CDO  
9 | interpolation was not mass conservative, but resulted in global  $O_2$  flux differences generally of  
10 | less than 1%. An exception was the CESM, whose output was converted conservatively to a  
11 | regular grid using a CESM-specific mapping file.

## 12 | 2.2 Atmospheric Transport Model Simulations

### 13 | 2.2.1 Matrix Method

14 | A matrix method was used to translate the ocean model air-sea  $O_2$ ,  $N_2$  and  $CO_2$  fluxes into  
15 | corresponding annual mean cycles in atmospheric potential oxygen (APO). The method was  
16 | based on the pulse-response functions from the Transcom 3 Level 2 (T3L2) atmospheric tracer  
17 | transport model (ATM) intercomparison. Each of the 13 ATMs that participated in T3L2  
18 | conducted forward simulations in which a uniformly distributed  $CO_2$  flux, normalized to  $1PgC$   
19 |  $yr^{-1}$ , was released from each of 11 ocean regions (Figure 1) for each of 12 “emission months,”  
20 | i.e., Jan-Dec, allowed to decay for 35 months, using an annually repeating cycle of meteorology  
21 | that was model specific for each ATM, and sampled every month at a range of surface  
22 | monitoring sites [*Gurney et al.*, 2003; 2004]. The APO code was developed from an earlier

Cynthia Nevison 10/27/2014 11:43 AM

Formatted: Subscript

Cynthia Nevison 10/27/2014 11:45 AM

Formatted: Subscript

Cynthia Nevison 10/27/2014 11:44 AM

Formatted: Subscript

Cynthia Nevison 10/21/2014 11:03 AM

Deleted: pattern

Cynthia Nevison 10/21/2014 11:06 AM

Deleted: A map of the Transcom regions  
can be found at  
[http://transcom.project.asu.edu/transcom03\\_protocol\\_basisMap.php](http://transcom.project.asu.edu/transcom03_protocol_basisMap.php).

1 pulse-response matrix code, which has been described in detail in *Nevison et al.* [2012b], that  
 2 translates terrestrial net ecosystem exchange (NEE) fluxes of carbon into the corresponding  
 3 annual mean cycles in atmospheric CO<sub>2</sub>. The matrix method is considerably faster than a full  
 4 forward ATM simulation, allowing annual mean cycles in APO from 13 different ATM<sub>s</sub> to be  
 5 computed in seconds, rather than the days or weeks required for a single forward simulation.

Cynthia Nevison 10/21/2014 11:17 AM  
 Deleted: d

Cynthia Nevison 10/27/2014 11:49 AM  
 Deleted: S

6 The pulse-response matrix code was applied separately to the O<sub>2</sub>, N<sub>2</sub> and oceanic CO<sub>2</sub> fluxes  
 7 from the last 12 years of the historical simulations, spanning 1994-2005, converting from carbon  
 8 to oxygen or nitrogen units where appropriate, to create three separate time series of atmospheric  
 9 O<sub>2</sub>, N<sub>2</sub> and CO<sub>2</sub> as mole fraction anomalies (μmol mol<sup>-1</sup>) on a H<sub>2</sub>O-free basis, where the O<sub>2</sub> and  
 10 N<sub>2</sub> anomalies are computed as though O<sub>2</sub> and N<sub>2</sub> were trace gases, similar to CO<sub>2</sub>. These were  
 11 combined to calculate a 9-year time series in APO in per meg units, spanning fluxes from 1997-  
 12 2005, according to Equation 1 [Stephens et al., 1998]:

$$APO = \frac{1}{X_{O_2}}(O_2) - \frac{1}{X_{N_2}}(N_2) + \frac{1.1}{X_{O_2}}(CO_2), \quad (1)$$

14 where X<sub>O<sub>2</sub></sub> and X<sub>N<sub>2</sub></sub> are the dry air mole fractions of O<sub>2</sub> and N<sub>2</sub> in H<sub>2</sub>O-free air, treated here as  
 15 constants (0.2094 and 0.7808, respectively). The mean seasonal cycle was computed by  
 16 detrending the time series with a 3<sup>rd</sup> order polynomial and then taking the average of the  
 17 detrended data for all Januaries, Februaries, etc. The matrix method involves calculating  
 18 separately the components of APO at each measurement site arising from fluxes from each ocean  
 19 region. These components are then summed to compute the net APO signal. The model  
 20 definition of APO in Equation 1 ignores contributions to APO from land biospheric exchanges at  
 21 ratios other than 1.1 and fossil fuel burning, but these are very small in comparison to oceanic  
 22 contributions on seasonal time scales [Manning and Keeling, 2006; Nevison et al., 2008].

Cynthia Nevison 10/21/2014 12:07 PM  
 Deleted: total

Cynthia Nevison 10/21/2014 1:30 PM  
 Deleted: 6

Cynthia Nevison 10/21/2014 1:30 PM  
 Deleted: 4

Cynthia Nevison 10/21/2014 12:08 PM  
 Deleted: the

Cynthia Nevison 10/21/2014 12:08 PM  
 Deleted: time

### 2.2.2 Evaluation of matrix method based on APO Transcom

An evaluation exercise was conducted in which the APO pulse-response matrix code was forced by climatological O<sub>2</sub> and N<sub>2</sub> fluxes from *Garcia and Keeling* [2001] and used to compute the mean seasonal cycle in APO as described above using Equation 1 (minus the oceanic CO<sub>2</sub> term).

The matrix-based results were evaluated against the mean seasonal cycles from archived station output from the forward ATM simulations of the APO Transcom Experiment, which also used the Garcia and Keeling O<sub>2</sub> and N<sub>2</sub> forcing fluxes [Blaine, 2005; Nevison et al., 2012b]. This evaluation was conducted using a subset of 9 of the original 13 T3L2 ATMs that also participated in APO Transcom. For this subset, the matrix method performed well in relatively

homogeneous regions like the Southern Ocean and at northern high latitude sites like Barrow, Alaska (BRW) and Alert, Canada (ALT). It was less reliable in capturing the forward simulation cycle at sites located within Northern midlatitude ocean regions, including Cold Bay, Alaska and La Jolla, California, where the uniform distribution of fluxes assumed by T3L2 did not accurately capture the impact of strong heterogeneity in air-sea fluxes from these regions

(Supplementary Tables S1, S2 and Supplementary Figures S1, S2). These same North Pacific stations are subject to large uncertainty in full forward ATM simulations due to uncertainty in vertical mixing [Stephens et al., 1998; Battle et al., 2006; Tohjima et al., 2012]. We therefore

focus in Section 3 on ALT, BRW and three Southern Ocean sites, including Macquarie Island (MQA), Palmer Station, Antarctica (PSA) and South Pole (SPO) in our use of APO to evaluate the ESM-simulated air-sea O<sub>2</sub>, N<sub>2</sub> and CO<sub>2</sub> fluxes. The locations of these 5 sites with respect to the T3L2 ocean regions is shown in Figure 1.

While the evaluation exercise indicates that the matrix method reproduces the shape and phase of the seasonal cycles with high reliability at the above sites, it tends to underestimate the seasonal

Cynthia Nevison 10/21/2014 12:14 PM  
Deleted: from

Cynthia Nevison 10/21/2014 12:19 PM  
Deleted: T

Cynthia Nevison 10/21/2014 12:17 PM  
Deleted: strong seasonal rectifier effects

Cynthia Nevison 10/28/2014 11:06 AM  
Deleted: several

1 amplitude by about 4-5% at ALT and BRW and by 11-12% at MQA and SPO and to slightly  
2 overestimate the amplitude at PSA. In applying the matrix code to the ESM oceanic fluxes, we  
3 therefore scaled up the estimated cycles by site and ATM-specific scaling factors obtained from  
4 the evaluation exercise (Supplemental Tables S1, S2, Supplemental Figure S2). Since these  
5 scaling factors were only available for ~~the~~ subset of 9 of the 13 T3L2 ATMs that also  
6 participated in APO Transcom, we subsequently (Section 3.1) compare observations  
7 alternatively to the scaled 9-model subset, or to all 13 unscaled models. ▼

Cynthia Nevison 10/21/2014 12:17 PM

Deleted: a

Cynthia Nevison 10/21/2014 12:21 PM

Deleted: original

Cynthia Nevison 10/21/2014 12:21 PM

Deleted: .

### 9 2.2.3 Component O<sub>2</sub> Fluxes

10 The net air-sea O<sub>2</sub> flux for each ESM can be divided into three components, associated with  
11 NCP, deep ventilation and thermal processes [Nevison *et al.*, 2012a]:

$$12 \quad F_{O_2, total} = F_{O_2, NCP} + F_{O_2, vent} + F_{O_2, therm} \quad (2)$$

13 These in turn can be used to force the matrix model and the resulting total APO cycle can be  
14 presented as the sum of component signals according to Equation 3.

$$15 \quad APO = APO_{NCP} + APO_{vent} + APO_{therm} \quad (3)$$

16 Here, the APO<sub>therm</sub> term also includes the effects of N<sub>2</sub> fluxes, as per the second right-hand term  
17 in Equation 1. The atmospheric signal due to oceanic CO<sub>2</sub> (last term in Equation 1) is not easily  
18 included in any of the component terms in Equation 3 based on available ESM output, but in  
19 principle all three component processes may lead to changes in CO<sub>2</sub> fluxes as well as O<sub>2</sub> fluxes.  
20 In practice, CO<sub>2</sub> has only a small influence on the amplitude and phasing of APO in most of the  
21 ESMs and thus is ignored in the component analysis. An exception is MPIM, in which the

1 oceanic CO<sub>2</sub> signal has a peak-to-trough seasonal amplitude of up to 5 ppm in the Southern  
2 Ocean that opposes the O<sub>2</sub> cycle, as noted previously [*Anav et al.*, 2013] and discussed further  
3 below.

4 Among the terms in Equation 2, F<sub>O<sub>2</sub>,total</sub> was provided outright by the ESMs and the thermal  
5 component F<sub>O<sub>2</sub>,therm</sub> can be derived easily from standard ESM output following the approach  
6 described above for N<sub>2</sub>. The remaining terms, F<sub>O<sub>2</sub>,NCP</sub> and F<sub>O<sub>2</sub>,vent</sub> are more challenging to  
7 estimate from available ESM output. In *Nevison et al.* [2012a], F<sub>O<sub>2</sub>,NCP</sub> was estimated from EP  
8 multiplied by a molar ratio of 1.4 mol O<sub>2</sub> per mol C exported. The assumption that F<sub>O<sub>2</sub>,NCP</sub> = 1.4  
9 EP was shown in *Nevison et al.* [2012a] to yield reasonable results for EP derived from satellite  
10 data (and indeed was applied to the satellite data described below in Section 2.3), but this  
11 approach proved unsatisfactory for EP<sub>100</sub> from the ESMs, especially in the Southern Ocean as  
12 discussed further below, since it yielded an atmospheric signal that was unreasonably small.  
13 The assumption also led to phasing uncertainties for some models (IPSL, NorESM1 and MPIM)  
14 that use finite sinking velocities for particulate organic carbon (as opposed to instantaneous  
15 vertical redistribution, as assumed, e.g., by CESM) with a resulting delay in EP<sub>100</sub> relative to  
16 NPP. Since the timing of F<sub>O<sub>2</sub>,NCP</sub> is likely to be more closely related to NPP than EP<sub>100</sub> [*Nevison*  
17 *et al.*, 2012a], we estimated F<sub>O<sub>2</sub>,NCP</sub> from the ESMs alternatively as 1.4EP<sub>100</sub> and 1.4 *ef*\* NPP,  
18 where NPP is the standard, vertically-integrated ESM output variable and *ef* is the model-specific  
19 annual mean EP<sub>100</sub>/NPP ratio, integrated over the 40-60°N or 40-60°S latitude band for northern  
20 and southern stations, respectively ([Table 1](#)).

21 Finally, F<sub>O<sub>2</sub>,vent</sub> in principle can be estimated as a residual of the other 3 terms in Equation 2.  
22 F<sub>O<sub>2</sub>,vent</sub> was estimated with reasonable success at the northern hemisphere sites, but generally  
23 looked unreasonable in the Southern Ocean for most models, with the exception of IPSL. The

1 signals were judged to be unreasonable on the basis of whether the  $\text{APO}_{\text{vent}}$  term, if estimated as  
2 a residual from Equation 3, dominated the  $\text{APO}_{\text{NCP}}$  term in driving the springtime rise in APO.  
3 In reality, the  $\text{APO}_{\text{NCP}}$  term must be primarily responsible for this rise [Keeling *et al.*, 1993;  
4 Bender *et al.*, 1996; Nevison *et al.*, 2012a]. We therefore do not attempt to explicitly resolve or  
5 present  $\text{APO}_{\text{vent}}$  signals in the Southern Hemisphere. While the problems with  $\text{APO}_{\text{vent}}$   
6 necessarily imply a corresponding problem in one or both of the other component terms  $\text{APO}_{\text{NCP}}$   
7 and  $\text{APO}_{\text{therm}}$ , as discussed below, the shape of these latter terms is still informative and is less  
8 sensitive to the uncertainties inherent in the residually-estimated  $\text{APO}_{\text{vent}}$  term.

### 11 2.3 Satellite Ocean Color Data

12 The primary output product of satellite ocean color measurements historically has been the  
13 concentration of chlorophyll-a (Chl), which is also the main input to most satellite-based ocean  
14 primary productivity models [Behrenfeld and Falkowski, 1997]. However, the standard Chl  
15 product based on empirical band-ratios of reflectances represents primarily the coefficient of  
16 total absorption of blue light and is inherently biased if the distributions of the optically active  
17 components deviate from the global “mean” [Lee *et al.*, 2011; Siegel *et al.*, 2005; Sauer *et al.*,  
18 2012]. In the Southern Ocean the standard Chl algorithms underestimate *in situ* Chl by 2-3 times  
19 [Mitchell & Kahru, 2009] whereas in the Arctic they overestimate it [Mitchell, 1992]. These  
20 errors are directly transferred into errors in estimates of net primary production (NPP) and export  
21 production (EP).

Cynthia Nevison 10/23/2014 11:26 AM

**Deleted:** Lacking a consistent method for estimating a reasonable  $\text{F}_{\text{O}_2, \text{vent}}$  term in both hemispheres using available ESM output, w

Cynthia Nevison 10/23/2014 11:26 AM

**Deleted:** this study

Cynthia Nevison 10/21/2014 12:39 PM

**Formatted:** Subscript

Cynthia Nevison 10/21/2014 12:40 PM

**Formatted:** Subscript

Cynthia Nevison 10/21/2014 12:40 PM

**Formatted:** Subscript

Cynthia Nevison 10/21/2014 12:48 PM

**Formatted:** Subscript

1 For the Southern Hemisphere we used an empirical Chl algorithm (SPGANT) that was tuned to  
2 in situ Chl in the Southern Ocean and spatially blended with the standard SeaWiFS OC4  
3 algorithm [Kahru and Mitchell, 2010]. The same blending scheme was applied when blending  
4 NPP between two versions of the Vertically Generalized Productivity Model (VGPM) algorithm  
5 [Behrenfeld & Falkowski, 1997]: the Southern Ocean version and the low-latitude version of  
6 Kahru *et al.* [2009]. EP was calculated using a modified version of the Laws [2004] model  
7 according to Nevison *et al.* [2012a]. The mean annual cycles for Chl, NPP and EP were  
8 calculated for 1997-2009 using data derived from SeaWiFS.

9  
10 For the Northern Hemisphere we used NPP data calculated according to the standard VGPM  
11 using MODIS-Aqua Chl. NPP was downloaded from  
12 <http://science.oregonstate.edu/ocean.productivity>. EP was calculated according to Dunne *et al.*  
13 [2005]. The mean annual cycles for NPP and EP were calculated for 2002-2011 using monthly  
14 composites derived from MODIS-Aqua. While the Laws [2004] and Dunne *et al.* [2005] methods of  
15 deriving EP are not identical, they both estimate export efficiency as a function of sea-surface  
16 temperature and NPP, are fitted to *in situ* data, and generally produce similar estimates. In Nevison *et*  
17 *al.* [2012a] the Southern Ocean EP derived with the Laws model was modified by constraining to the  
18 bulk nutrient budget estimated in the ocean inversion of Schlitzer [2000]. That reduced the  
19 unrealistically high export efficiency of the Laws model observed at cold temperatures and brought it  
20 into closer agreement with the Dunne *et al.* export efficiency.

21 Both the SPGANT and VGPM/OSU satellite algorithms for NCP were converted to air-sea O<sub>2</sub>  
22 fluxes using  $F_{O_2,NCP} = 1.4 \text{ NCP}$ , where 1.4 refers to the molar ratio between O<sub>2</sub> produced and  
23 carbon fixed in photosynthesis.  $F_{O_2,NCP}$  was used to force the pulse-response code to estimate the  
24 corresponding APO signal associated with NCP as per Nevison *et al.* [2012a].

Cynthia Nevison 10/27/2014 12:30 PM  
**Deleted:** and

Cynthia Nevison 10/21/2014 3:13 PM  
**Formatted:** Font:Italic

Cynthia Nevison 10/21/2014 3:13 PM  
**Formatted:** Font:Italic

Cynthia Nevison 10/21/2014 3:16 PM  
**Formatted:** Font:Italic

Cynthia Nevison 10/21/2014 3:14 PM  
**Formatted:** Font:Italic

Cynthia Nevison 10/21/2014 3:14 PM  
**Formatted:** Font:Italic

Cynthia Nevison 10/21/2014 3:15 PM  
**Formatted:** Font:Italic

## 2.4 APO Data

APO is a unique atmospheric tracer of ocean biogeochemistry that is calculated by combining high precision O<sub>2</sub> and CO<sub>2</sub> data according to  $APO = O_2 + 1.1CO_2$  [Stephens *et al.*, 1998]. By design, APO is mostly insensitive to exchanges with the land biosphere, which have a nearly fixed stoichiometry that produces compensating changes in O<sub>2</sub> and CO<sub>2</sub>. In contrast, the exchanges of O<sub>2</sub> and CO<sub>2</sub> across the air-sea interface are not strongly correlated, largely because variability in dissolved CO<sub>2</sub> is strongly damped by carbonate chemistry in seawater on seasonal timescales. As a result, seasonal variability in APO reflects changes in atmospheric oxygen occurring almost solely due to oceanic processes [Manning and Keeling, 2006].

Atmospheric O<sub>2</sub> data, reported in terms of deviations in the O<sub>2</sub>/N<sub>2</sub> ratio, were obtained from the Scripps Institution of Oceanography (SIO) and Princeton University (PU) networks. Data are available from the early to mid 1990s, depending on the station [Bender *et al.*, 2005; Manning and Keeling, 2006]. In Figure 2, we use SIO data from SPO, PSA and ALT and PU data from MQA and BRW. Details of the station locations and time spans of data used to calculate the mean seasonal cycle are listed in Table S2 and shown in Figure 1. For MQA (1997-2007) and BRW (1993-2008), the time spans overlapped mostly but not perfectly with the CMIP5 model output (1994-2005) and the satellite data (1997-2009 for SPGANT, 2002-2011 for VGPM).

APO was calculated according to,

$$APO = \delta(O_2/N_2) + \frac{1.1}{X_{O_2}} CO_2, \quad (4)$$

where  $\delta(O_2/N_2)$  is the relative deviation in the O<sub>2</sub>/N<sub>2</sub> ratio from a reference ratio in per meg units,  $X_{O_2} = 0.2094$  is the O<sub>2</sub> mole fraction of dry air [Tohjima *et al.*, 2005], CO<sub>2</sub> is the mole fraction of carbon dioxide in parts per million (μmol mol<sup>-1</sup>), and 1.1 is a qualitative estimate of the -O<sub>2</sub>:C

Cynthia Nevison 10/21/2014 1:16 PM

Deleted: data

Cynthia Nevison 10/21/2014 3:22 PM

Deleted: Details of the station locations are listed in Table S2.

Cynthia Nevison 10/27/2014 2:19 PM

Deleted: 1

Cynthia Nevison 10/21/2014 1:29 PM

Deleted: 5

Cynthia Nevison 10/21/2014 1:29 PM

Deleted: Stephens

Cynthia Nevison 10/21/2014 1:29 PM

Deleted: 1998

Cynthia Nevison 10/21/2014 1:22 PM

Deleted: the average

ratio of terrestrial respiration and photosynthesis. Mean seasonal cycles for observed APO were obtained using the same detrending and averaging methodology described in Section 2.2.1. The uncertainty in the observed mean seasonal cycles over the timespan of available data is less than 6% at extratropical latitudes, reflecting a combination of instrumental precision, synoptic variability and interannual variability (IAV) in the seasonal cycle. The current study is focused on the mean seasonal cycle in APO as a first order challenge for the CMIP5 ocean models. Here, model, APO and satellite seasonal cycles are evaluated over roughly comparable periods that are dictated by data availability. The examination of interannual variability is deferred to future research, which will require ATM simulations of APO driven by interannually varying meteorology.

## 2.5 Phase Metrics

The time of year of the seasonal maximum in APO and NPP was used as a phase metric. For APO, monthly mean, station-specific time series, both modeled and observed, were fit to a 3<sup>rd</sup> order polynomial plus first 2 harmonics function. The harmonic components of the fit were used to construct a mean seasonal cycle with daily resolution and the day of the seasonal maximum was identified. The same approach was used to derive the day of the seasonal NPP maximum, except that the fit was applied to monthly mean satellite-derived and ESM NPP integrals summed from 40-60°S and 40-60°N, which were compared to the APO phase metric at southern and northern stations, respectively.

## 3. Results

### 3.1 APO comparison to Earth System Models

Cynthia Nevison 10/21/2014 3:26 PM

**Deleted:**

Cynthia Nevison 10/21/2014 3:26 PM

**Deleted:** small

Cynthia Nevison 10/21/2014 3:27 PM

**Deleted:** , such that these are presented without error bars in Figure 1

Cynthia Nevison 10/22/2014 2:36 PM

**Deleted:** Varying the number of harmonic terms in the fit from 1 to 4 yielded a maximum that generally fell within  $\pm 5$  days of the standard 2-harmonic fit maximum, providing a measure of the uncertainty in the phase metric.

1 The APO cycles estimated from the 6 [sets of](#) ESM air-sea fluxes were compared to observations  
2 at 3 Southern Ocean and 2 northern monitoring sites (Figure [2](#)). In these plots, the green  
3 envelope reflects our best estimate of the ATM uncertainty in the ocean model APO signal based  
4 on the 9 scaled ATM results, while the gray window reflects the more complete range of  
5 uncertainty using all 13 unscaled ATM results. In general, the distinction between the green and  
6 gray windows is only moderately important, as the observed APO cycle in most cases either falls  
7 within both envelopes or lies outside of both envelopes.

8 The MPIM and related NorESM1 ocean biogeochemistry models are examples in which the  
9 observed APO cycle lies outside both ranges of uncertainty at all 5 evaluation sites (Figure [2](#),  
10 lower middle and right panels). For these models, the rise in the APO cycle occurs too early in  
11 the springtime in both hemispheres, while the overall amplitude of the cycle is too large at all the  
12 southern stations. Here, it is notable that the MPIM APO amplitude would be even larger in the  
13 Southern Ocean if it were not offset by the unrealistically large seasonal cycle in oceanic CO<sub>2</sub>  
14 described above. The large CO<sub>2</sub> cycle, however, does not substantially alter the phase of APO,  
15 which is determined mainly by the timing of the O<sub>2</sub> fluxes.

16 IPSL is another ocean biogeochemistry model for which the observed APO cycle lies outside of  
17 both the best guess and full range of uncertainty at all monitoring sites, with the exception of  
18 Palmer Station (64.9°S), where observed APO falls within the wider gray window of uncertainty  
19 (Figure [2b](#), lower left panels). Unlike MPIM and NorESM1, the rise in the IPSL APO cycle  
20 occurs somewhat later in the springtime than observed, while the overall amplitude of the cycle  
21 tends to be underestimated. The underestimate is mild at all the southern stations, and even falls  
22 within the broader range of uncertainty at PSA, but is more pronounced at the northern  
23 monitoring sites, where the IPSL amplitude is too small by nearly a factor of 2.

Cynthia Nevison 10/27/2014 2:19 PM  
Deleted: 1

Cynthia Nevison 10/27/2014 2:19 PM  
Deleted: 1

Cynthia Nevison 10/27/2014 2:19 PM  
Deleted: 1

1 CESM is the top-performer among the 6 ESMs evaluated, consistently yielding green (gray)  
2 windows that encompass the observed APO cycle at most (all) of the 5 monitoring sites (Figure  
3 2, upper left panels). GFDL ESM2M (depth-based coordinates) is the second most consistent  
4 performer, yielding cycles that generally agree with observations, with exceptions at BRW,  
5 where ESM2M tends to mildly underestimate the depth of the APO trough, and at PSA, where  
6 the rise in the APO cycle may be up to 1 month too early. The sigma-coordinate GFDL ESM2G  
7 model is the third best performer, capturing the observed APO cycle relatively well at most  
8 southern stations, but underestimating the seasonal amplitude at the northern stations.

### 9 3.1.1 Regional analysis of APO cycle

10 The matrix method can partition the ocean model APO cycles into regional contributions from  
11 the 11 ocean regions used in T3L2. At the southern stations of SPO, PSA, and MQA, this  
12 partitioning reveals, not surprisingly, that the Southern Ocean (defined as all ocean regions south  
13 of 44°S) dominates the APO cycle (not shown). However, at BRW and ALT at least 3 regions  
14 make important contributions, including the “temperate” North Pacific (extending from 15°N to  
15 the Bering Strait around 65°N and thus including the subpolar region), the “temperate” North  
16 Atlantic (extending from 15°N to 48°N) and the “Northern Ocean” (including the Arctic Ocean  
17 and the North Atlantic north of 48°N). The Northern Ocean is the most important contributor to  
18 the APO seasonal cycle at both BRW (Figure 3) and ALT and is by far the most variable  
19 component among the 6 ESMs. The largest Northern Ocean APO amplitudes are produced by  
20 CESM and NorESM1, which are the only two models that capture the total observed APO  
21 amplitude at BRW (Figure 2d).

Cynthia Nevison 10/23/2014 10:13 AM

Deleted: /

Cynthia Nevison 10/23/2014 10:13 AM

Deleted: /

Cynthia Nevison 10/27/2014 2:20 PM

Deleted: 1

Cynthia Nevison 10/23/2014 10:15 AM

Deleted: ranscom

Cynthia Nevison 10/23/2014 10:13 AM

Deleted: 5

Cynthia Nevison 10/27/2014 2:18 PM

Deleted: 2

Cynthia Nevison 10/23/2014 10:17 AM

Deleted: signal

Cynthia Nevison 10/23/2014 10:18 AM

Deleted: seen for

Cynthia Nevison 10/23/2014 10:19 AM

Deleted: reproduce

Cynthia Nevison 10/27/2014 2:20 PM

Deleted: 1

1    **3.1.2 Partitioning of APO cycle among component signals**

2    To probe further into the underestimate of the APO amplitude at BRW by most of the ESMs, we  
3    partitioned APO into thermal and NCP-related components, as described in Section 2.2.3 (Figure  
4    4). A comparison of CESM and ESM2M in Figure 4 indicates that both have similar  $APO_{\text{therm}}$   
5    and  $APO_{\text{NCP}}$  signals, but that CESM captures total APO more or less correctly while ESM2M  
6    underestimates the total APO amplitude. By inference, the missing  $APO_{\text{vent}}$  term accounts for  
7    the difference. However, as discussed in Section 2.2.3,  $APO_{\text{vent}}$  can be estimated only as a  
8    residual of 3 other terms using standard CMIP5 output and thus its shape and phasing are  
9    sensitive to even small uncertainties in those other terms. Thus, the residual ventilation curves in  
10   Figure 4 should be interpreted with caution (e.g., the MPIM curve is clearly unreasonable in  
11   phasing). The four remaining ESMs have  $APO_{\text{NCP}}$  cycles of similar or smaller amplitude than  
12   CESM, which in the case of ESM2G and MPIM is due primarily to their relatively low ef-ratios,  
13   and all these models substantially underestimate the total APO amplitude at BRW. This suggests  
14   that these models probably also underestimate some combination of deep ventilation and NCP.  
  
15   A similar partitioning of APO was attempted in the Southern Ocean, but the estimation of  
16    $APO_{\text{NCP}}$  from model EP<sub>100</sub> generally did not give plausible results in this region. This problem is  
17   discussed in more detail in Section 4.

18   **3.2 Satellite data compared to ESMs**

19   Estimates of net primary production display a wide variety of spatial patterns among models and  
20   satellite data (Figure 5). Global totals range over more than a factor of 2 (34-82 Pg C/yr) among  
21   the ESMs, with most models tending to exceed the VGPM satellite-based estimate of 45 Pg C/yr  
22   (Table 1). Global EP is more consistent among the models, with a value around 8 Pg C/yr in

Cynthia Nevison 10/27/2014 2:18 PM

Deleted: 3

Cynthia Nevison 10/27/2014 2:18 PM

Deleted: 3

Cynthia Nevison 10/23/2014 10:35 AM

Deleted: (

Cynthia Nevison 10/23/2014 10:35 AM

Deleted: A

Cynthia Nevison 10/23/2014 10:41 AM

Deleted: is

Cynthia Nevison 10/23/2014 11:36 AM

Deleted: not presented in Figure 3 due to difficulties in resolving this residual term consistently across APO monitoring sites using standard ESM output).

Cynthia Nevison 10/27/2014 2:17 PM

Deleted: 4

1 most cases, in good agreement with the satellite-based estimate. Global EP converges among the  
2 ESMs because the model with highest global NPP (ESM2M) has a small ef-ratio of  $< 0.1$  and the  
3 models with lowest global NPP (IPSL, NorESM1) have the largest ef-ratios of about 0.2 (Table  
4 1).

5 The high global NPP totals in the ESMs are driven in large part by high tropical NPP values,  
6 which generally are not reflected in the satellite data except along coastlines (Figure 5). In this  
7 paper, we focus on the 40-60° latitude bands, which are more important than the tropics in  
8 driving the seasonal cycles in NPP, EP (NCP) and APO [Garcia and Keeling, 2001; Anav et al.,  
9 2013]. In the Southern Ocean 40-60°S band, global NPP ranges among ESMs from 5.2 to 12.5  
10 PgC/yr, encompassing the satellite-based estimates (Table 1, Figure 6). However, the ESMs  
11 tend to underestimate EP relative to the satellite-derived values, particularly the SPGANT/Laws  
12 product, due largely to the small model ef-ratios. In the 40-60°N band, the ESMs generally  
13 underestimate both NPP and ef-ratios relative to the satellite-derived values. This combination  
14 leads to model EP values that are smaller than satellite EP by a factor of 2 on average (Table 1).  
15 In both hemispheres, the model NPP maximum tends to occur earlier than the satellite-derived  
16 maximum, with some models (IPSL, MPIM) predicting a maximum that is up to 1-2 months  
17 early (Figure 6).

### 18 3.3 Combining APO and Satellite Data

19 In the previous sections we considered APO and satellite data as separate evaluation metrics for  
20 ESMs. Below we consider the two as combined metrics. While this analysis is limited by  
21 uncertainties in the absolute magnitude of satellite NPP and EP/NCP and our imperfect ability to

Cynthia Nevison 10/27/2014 2:17 PM  
Deleted: 4

Cynthia Nevison 10/27/2014 2:16 PM  
Deleted: 5

Cynthia Nevison 10/27/2014 2:16 PM  
Deleted: 5

partition the ESM total APO signal into its NCP and other components, it nevertheless provides some additional insight into the behavior of the ESMs.

### 3.3.1 Phase metrics

The phase metrics [defining the timing of the observed and model seasonal maximum in APO](#) reveal characteristic patterns for each ESM, which are relatively consistent across APO monitoring sites ([Figure 7](#)). The APO seasonal maxima of MPIM and NorESM1 are earlier than observed by about 1 month and 3 weeks, respectively, on average, while the IPSL APO maximum (with the exception of PSA) tends to be later than observed by 2-3 weeks. The remaining models, CESM, ESM2M and ESM2G, have seasonal APO maxima that are relatively consistent with observations, although with some variation among different stations.

The observed seasonal maximum of NPP occurs about 30-40 days earlier than the observed APO maximum in the Southern Ocean stations and about 50 days earlier at BRW and ALT. Of the models, ESM2G, CESM and ESM2M capture the phase of the NPP maximum to within about 1-3 weeks, although as noted above in [Figure 6](#), the model NPP maxima tend to occur earlier than the satellite-based maxima. In MPIM, the NPP maximum is about 1 to 1.5 months earlier than observed, and the APO maximum is also corresponding early ([Figure 7](#)). IPSL is an outlier from the general slope of the APO vs. NPP phase relationship, as defined by the rest of the ESMs. The IPSL NPP maximum occurs about 40 days earlier than observed in the Southern Hemisphere and nearly 2 months earlier than observed in the Northern Hemisphere, but IPSL, curiously, also has the latest APO seasonal maximum of any of the models. NorESM1 is another outlier in the opposite direction off the general APO vs. NPP phase slope, at least in the Northern Hemisphere. There, NorESM1's seasonal maximum in NPP has a relatively small lag from the APO

Cynthia Nevison 10/23/2014 1:37 PM  
Deleted: (Figure 6)

Cynthia Nevison 10/27/2014 2:16 PM  
Deleted: 5

Cynthia Nevison 10/23/2014 1:35 PM  
Deleted: (Figure 6)

1 maximum compared to the other models. NorESM1 is also unusual in that the  $APO_{\text{therm}}$  seasonal  
2 maximum at Barrow occurs about 1 month later than in any of the other ESMs (Figure 4).

Cynthia Nevison 10/27/2014 2:17 PM  
Deleted: 3

### 3 3.3.2 Seasonal amplitudes

4 In addition to evaluating the phasing of the ocean model APO and NPP cycles, we examined the  
5 amplitude of the cycles, with the caveat that the absolute magnitude of satellite-based NPP is not  
6 well determined and at present provides a relatively weak constraint on the models.

7 Furthermore, the APO seasonal amplitude in principle is more closely related to NCP (or EP)  
8 than NPP. However, we chose NPP for the seasonal amplitude analysis due to the strong  
9 discrepancies in ef-ratio among models and satellite data indicated in Table 1, which may unduly  
10 bias the results.

11 A cross plot of the seasonal amplitude in APO against the seasonal amplitude of NPP integrated  
12 between 40-60°S suggests a strong correlation between the amplitudes of APO and NPP among  
13 the ocean biogeochemistry models, with larger NPP amplitudes associated with larger APO  
14 cycles. The strong correlation holds at all Southern Ocean stations and is illustrated in Figure 8a  
15 at Macquarie. The cluster of top-performing ESMs (CESM, ESM2M, ESM2G) agrees relatively  
16 well with the observed APO and SPGANT amplitudes. Meanwhile both amplitudes are  
17 underestimated by IPSL and overestimated by NorESM1 and MPIM.

Cynthia Nevison 10/27/2014 2:14 PM  
Deleted: 7

18 Cross plots of the seasonal amplitudes of APO and NPP in the northern hemisphere reveals that  
19 these amplitudes are positively correlated at BRW (Figure 8b) and ALT (not shown), although  
20 the correlation is weaker than in the Southern Hemisphere. CESM, ESM2G, ESM2M and MPIM  
21 all capture the satellite-based NPP seasonal amplitude relatively well, while both CESM and

Cynthia Nevison 10/27/2014 2:14 PM  
Deleted: 7

1 NorESM1 capture the observed APO amplitude accurately. However, CESM is the only model  
2 that reproduces both the NPP and APO seasonal amplitudes well relative to the observations.

### 3 4. Discussion

#### 4 4.1 Northern Ocean

5 Most ESMs tend to underestimate substantially the observed seasonal amplitude of APO at  
6 Barrow, Alaska. A combination of region-specific results (Figure 3) and O<sub>2</sub> component analysis  
7 (Figure 4) suggests that some combination of fall/winter deep ventilation and spring/summer  
8 export production in the Northern Ocean (defined to include the North Atlantic north of 48°N) in  
9 particular may be underestimated in many models. The combined analysis of the APO vs. NPP  
10 seasonal amplitudes (Figure 8b) supports these conclusions and suggests that, while several  
11 models may be capturing primary production well in the Northern Ocean, accurate representation  
12 of export production and deep ventilation is also important for reproducing the observed APO  
13 cycle. The inference from the APO component analysis in Figure 4 that the GFDL models may  
14 have weak ventilation in the North Atlantic appears to contradict the analysis of Dunne et al.  
15 [2012], who found robust NADW formation in both the ESM2M and ESM2G versions, but  
16 possibly could be reconciled if the biogeochemical gradients across which deep water formation  
17 acts are too weak.

18 We investigated several mechanisms that might explain the differences among models in the  
19 APO cycle at high northern latitudes, including subpolar heat transport and Arctic sea ice cover.  
20 Here, stronger northward heat transport should lead to more deep ventilation, while lower sea ice  
21 cover will permit more production and ventilation in the Arctic Ocean. Subdividing the  
22 Northern Ocean region into Arctic Ocean and North Atlantic components revealed that some

Cynthia Nevison 10/27/2014 2:18 PM

Deleted: 2

Cynthia Nevison 10/27/2014 2:17 PM

Deleted: 3

Cynthia Nevison 10/23/2014 1:50 PM

Deleted: ing

Cynthia Nevison 10/27/2014 2:14 PM

Deleted: 7

Cynthia Nevison 10/27/2014 12:25 PM

Deleted: is not easily reconciled, however, with

Cynthia Nevison 10/23/2014 1:52 PM

Deleted: finding

Cynthia Nevison 10/23/2014 1:52 PM

Deleted: report

Cynthia Nevison 10/27/2014 12:27 PM

Deleted: Still, the stronger Atlantic overturning reported by Dunne et al. for ESM2M relative to ESM2G appears consistent with the larger APO amplitude predicted for ESM2M relative to ESM2G (Figure 1d)

Cynthia Nevison 10/28/2014 11:10 AM

Deleted: additional

1 models (IPSL and ESM2G) have a very small component ( $< 2$  per meg) of APO seasonal  
2 amplitude coming from the Arctic Ocean alone (Figure 9). In ESM2G this may be related to the  
3 extensive winter sea ice cover, which exceeds the observed covered area reported by the  
4 National Snow and Ice Data Center ([http://nsidc.org/data/seaice\\_index/archives.html](http://nsidc.org/data/seaice_index/archives.html)) by about 2  
5  $\times 10^6$  km<sup>2</sup>. However, sea ice cover is lower than observed in IPSL, suggesting the small Arctic  
6 APO component in that model is more related to general underestimate of primary and export  
7 production (e.g., as shown in Figures 6b and 8b). While it seems clear that the strong APO  
8 seasonality in CESM can be attributed in part to its high productivity and EP in the northern  
9 subpolar and polar regions (Figure 6 and Table 1), a full explanation for the underlying  
10 mechanisms of the CESM fidelity on APO compared to the other models is not readily apparent  
11 from surface-only data. This suggests the need for a more detailed exploration of ocean interior  
12 ventilation and biological response interactions outside the scope of the present work.

#### 13 4.2 Southern Ocean

14 Compared to the Northern Hemisphere stations, the ESMs generally are more successful in the  
15 Southern Ocean in capturing the observed APO cycle (Figure 2). Within the range of ATM  
16 uncertainty, at least 3 models, CESM, ESM2M, ESM2G (and IPSL at Palmer Station), predict  
17 seasonal APO amplitudes in agreement with observations. Although the Southern Ocean APO  
18 amplitude in these models varies over as much as 20 per meg, we currently are not able to  
19 distinguish which of the underlying air-sea O<sub>2</sub> flux fields is the most realistic, due to the  
20 uncertainty associated with translating these fluxes into an atmospheric signal using TransCom3  
21 era model responses to uniformly distributed regional fluxes. However, even with our current  
22 matrix method, the APO constraint is sufficiently robust to indicate that NorESM1 and MPIM  
23 substantially overestimate some combination of production and deep ventilation in the Southern

Cynthia Nevison 10/27/2014 2:13 PM  
Deleted: 8

Cynthia Nevison 10/23/2014 1:54 PM  
Deleted: (Figure 9)

Cynthia Nevison 10/27/2014 2:13 PM  
Deleted: 5

Cynthia Nevison 10/27/2014 2:13 PM  
Deleted: 7

Cynthia Nevison 10/27/2014 2:16 PM  
Deleted: 5

Cynthia Nevison 10/27/2014 2:19 PM  
Deleted: 1

Cynthia Nevison 10/28/2014 11:30 AM  
Deleted: accurate

Cynthia Nevison 10/23/2014 2:51 PM  
Formatted: Font:(Default) Times New Roman, 12 pt

1 Ocean, while IPSL probably tends to underestimate these fluxes (Table 1, Figure 8a). Notably,  
2 the ESMs that reproduce APO the best in the Southern Ocean tend to predict a smaller net  
3 carbon uptake between 44-75° and are in better agreement with independent estimates [Lenton  
4 et al., 2013] of carbon uptake from ocean inversions and observed pCO<sub>2</sub> databases (Figure 10).  
5 Reducing ATM uncertainty is a challenge that potentially can be addressed by using column-  
6 integrated APO signals from aircraft data [Wofsy et al., 2011], or conversely, by using vertical  
7 profiles to identify top-performing ATMs [Stephens et al., 2007]. In addition, the spread in  
8 ATM results has been reduced substantially for CO<sub>2</sub> inversions using post-Transcom3-era ATMs  
9 [Peylin et al., 2013], suggesting that ATM uncertainty also may be reduced for forward  
10 simulations of APO. If this is the case, then new forward simulations with several different  
11 modern-era ATMs may be sufficient to characterize ATM uncertainty. Alternatively, it may be  
12 valuable to continue with a matrix-based approach, using basis functions from many ATMs, but  
13 with redefined regional boundaries that are not defined based simply on latitude, as in T3L2  
14 (Figure 1), but rather that correspond to the biogeography of major ocean regions [Fay and  
15 McKinley, 2014]. The definition of such basis functions could help extend the utility of the  
16 matrix approach to lower latitude APO monitoring sites and allow for the partitioning of the  
17 Southern Ocean into multiple regions defined around biogeochemical function, while still  
18 retaining the advantages of the matrix method, i.e., the ability to quickly and easily compare  
19 multiple ATMs forced with the same air-sea fluxes.  
20 A second complication in the Southern Ocean analysis is that the EP<sub>100</sub> values reported by the  
21 ESMs clearly are not directly comparable to satellite NCP(EP) data, particularly our SPGANT  
22 product, and thus can not be translated with confidence into air-sea O<sub>2</sub> fluxes associated with  
23 NCP. A likely problem is that the 100 m depth horizon used to compute EP may not be

Cynthia Nevison 10/27/2014 2:14 PM

Deleted: 7

Cynthia Nevison 10/24/2014 9:53 AM

Formatted: Font:Times New Roman, 12 pt

Cynthia Nevison 10/24/2014 9:53 AM

Formatted: Font:Times New Roman, 12 pt

Cynthia Nevison 10/24/2014 9:53 AM

Formatted: Font:Times New Roman, 12 pt

Cynthia Nevison 10/24/2014 9:53 AM

Formatted: Font:Times New Roman, 12 pt

Cynthia Nevison 10/24/2014 9:53 AM

Formatted: Font:Times New Roman, 12 pt

Cynthia Nevison 10/24/2014 9:53 AM

Formatted: Font:Times New Roman, 12 pt

Cynthia Nevison 10/24/2014 9:53 AM

Formatted: Font:Times New Roman, 12 pt

Cynthia Nevison 10/24/2014 9:53 AM

Formatted: Font:Times New Roman, 12 pt

Cynthia Nevison 10/24/2014 10:00 AM

Formatted: Subscript

Cynthia Nevison 10/24/2014 9:53 AM

Formatted: Font:Times New Roman, 12 pt

Cynthia Nevison 10/28/2014 11:30 AM

Deleted: challenging problem

Cynthia Nevison 10/23/2014 2:19 PM

Deleted: as more

Cynthia Nevison 10/23/2014 2:19 PM

Deleted: become available

Cynthia Nevison 10/23/2014 2:22 PM

Deleted:

Cynthia Nevison 10/23/2014 2:23 PM

Formatted: Subscript

Cynthia Nevison 10/23/2014 2:24 PM

Formatted: Font:Italic

Cynthia Nevison 10/28/2014 11:20 AM

Formatted: Font:Italic

Cynthia Nevison 10/23/2014 2:55 PM

Deleted: readily

1 comparable across satellite algorithms and ocean biogeochemistry models.  $EP_{100}$  will  
2 underestimate the model's true NCP-related  $O_2$  outgassing flux if organic matter is respired as it  
3 sinks from the actual model mixed layer depth to 100m depth [Najjar *et al.*, 2007]. It is also  
4 puzzling that the ef-ratios predicted by the ESMs (Table 1) appear to have decreased  
5 considerably in some cases relative to those reported for earlier versions of the same models  
6 [Steinacher *et al.*, 2010]. For example, the Southern Ocean ef-ratios for MPIM and IPSL in that  
7 earlier study were about 0.2 and 0.4, respectively, compared to 0.14 and 0.27, respectively, in the  
8 current study. The mean global ef-ratio for the 6 ESMs in the current study is only 0.14 and,  
9 even in the Southern Ocean, is only 0.17 on average, compared to satellite-based estimates of  
10 0.18 globally and about 0.3 at high latitudes.

11 The small ef-ratios in the GFDL models (of less than 0.1 globally and only 0.10 to 0.13 in the  
12 Southern Ocean) appear consistent with the relatively deep summer MLDs in the Southern  
13 Ocean, which even at their minimum are often deeper than 100 m in both ESM2M and ESM2G  
14 [Dunne *et al.*, 2012]. In CESM the Southern Ocean summer mixed layer depths (MLDs) are  
15 generally shallower than 100 m and in many regions are only around 10-40 m deep [Moore *et*  
16 *al.*, 2013]. The shallower summer MLDs may contribute to CESM's larger ef-ratio of 0.18,  
17 although this ratio is still small compared to the satellite-based estimates. The small GFDL ef-  
18 ratios may also be related to an overvigorous picophytoplankton component wherein a  
19 prochlorococcus-like form is capable of competing relatively well even in cold polar waters. Small  
20 picophytoplankton are more likely to be reoxidized and remineralized within the mixed layer,  
21 whereas larger, heavier microphytoplankton (e.g., diatoms) are more likely to be exported out of  
22 the oceanic mixed layer [Uitz *et al.*, 2010].

### 23 4.3 Phase relationships

Cynthia Nevison 10/23/2014 2:55 PM

Deleted: (MPIM, IPSL)

Cynthia Nevison 10/23/2014 3:35 PM

Formatted: Font:12 pt

1 While much of our analysis focuses on the seasonal amplitude of APO and NPP at mid to high  
2 latitudes, both of these metrics involve relatively large uncertainty. This derives from  
3 [Transcom3-era uniform flux](#) ATM uncertainty in the case of APO, while for NPP the uncertainty  
4 results from the lack of strong constraints on the absolute magnitude of the satellite fluxes. In  
5 contrast, we have relatively high confidence in the phasing of model APO, as represented by the  
6 matrix method (see Supplementary Information) and in NPP observationally derived from  
7 satellite data, based on the close correspondence in phasing between the SPGANT and VGPM  
8 algorithms. For these reasons, we used a phase metric, i.e., the timing of the seasonal maximum,  
9 to examine relationships between observed and model APO and NPP. As in the seasonal  
10 amplitude analysis, MPIM, NorESM1, and IPSL displayed phasing patterns that tended to  
11 deviate from observations and the other three top-performing models, albeit in diverging ways.  
12 A complete diagnosis of the model physics responsible for the phasing anomalies (e.g., IPSL's  
13 early NPP maxima and late APO maxima) described in Section 3.3.1 is beyond the scope of this  
14 paper. Here we note mainly that the phase metrics are a robust and relatively good indicator of  
15 overall model performance with respect to APO.

## 16 5. Summary

17 We have used measurements of the seasonal cycles in APO to challenge and test the ocean  
18 model components of 6 ESMs. The model/data comparison reveals that [three](#) of the ESMs  
19 tested reproduce the observed cycles reasonably well, within the range of ATM uncertainty,  
20 while [three](#) do not. ESM performance in general is more favorable in the Southern Hemisphere  
21 than in the Northern Hemisphere, where most models appear to underestimate the wintertime  
22 ventilation of O<sub>2</sub>-depleted deepwater that drives the declining branch of the APO seasonal cycle  
23 and many may also underestimate both primary and export production, particularly at high

Cynthia Nevison 10/28/2014 11:35 AM

Deleted:

Cynthia Nevison 10/28/2014 11:36 AM

Deleted: half

Cynthia Nevison 10/28/2014 11:35 AM

Deleted: ESM

Cynthia Nevison 10/28/2014 11:36 AM

Deleted: half

1 northern latitudes. We used NPP and NCP(EP) products derived from satellite ocean color data  
2 as complementary constraints on the models in an effort to tighten the APO constraint, which  
3 reflects a combination of production and ventilation processes. However, while the satellite data  
4 provide relatively strong constraints with respect to phasing, they are more uncertain with respect  
5 to the absolute magnitudes of NPP and NCP(EP).

6 At least two primary uncertainties limit our ability to place stronger constraints on ocean model  
7 biogeochemistry based on currently available information from APO and satellite data: 1) The  
8 relatively large ATM uncertainty involved in translating air-sea O<sub>2</sub> fluxes into APO signals. 2)  
9 The uncertainty in how model EP<sub>100</sub> relates to the true model F<sub>O<sub>2</sub>,NCP</sub> flux and how this

10 relationship varies across models and satellite algorithms. The first of these, ATM uncertainty,

11 is large, as quantified using our Transcom3-based matrix method. However, it probably has

12 been overstated in previous analyses, which in some cases went so far as to suggest that APO

13 does not provide a useful constraint on ocean model fluxes [e.g., Naegler *et al.*, 2007]. Further,

14 ATM uncertainty could be reduced substantially in future work with modern ATMs and O<sub>2</sub>-

15 specific flux patterns, or with new regional boundaries defined based on ocean biogeography

16 rather than simple latitude. Even within the limits of our current approach, we have shown that

17 half of the 6 ESMs tested here produce APO cycles whose mismatch with observed APO clearly

18 transcends ATM uncertainty, suggesting underlying deficiencies in those models' physics and

19 biogeochemistry.

20 Improving the understanding of the relationship between model air-sea O<sub>2</sub> fluxes and quantities

21 like NPP, NCP and EP is a more tractable problem that can be dissected with appropriate model

22 diagnostics, e.g., as per Manizza *et al.* [2012]. In the current analysis, using standard CMIP5

23 output from 6 ocean biogeochemistry models, we encountered difficulties in relating F<sub>O<sub>2</sub></sub> to EP

Cynthia Nevison 10/28/2014 12:02 PM

Deleted: among

Cynthia Nevison 10/23/2014 3:45 PM

Deleted: substantial

Cynthia Nevison 10/28/2014 12:03 PM

Deleted: but

Cynthia Nevison 10/28/2014 12:03 PM

Deleted: also

Cynthia Nevison 10/28/2014 11:40 AM

Formatted: Font:12 pt

Cynthia Nevison 10/23/2014 3:43 PM

Formatted: Subscript

Cynthia Nevison 10/28/2014 11:39 AM

Deleted: .

Cynthia Nevison 10/28/2014 11:48 AM

Deleted: W

Cynthia Nevison 10/28/2014 11:58 AM

Formatted: Subscript

1 | and NCP, which hindered our ability to diagnose the mechanisms responsible for model  
2 | performance and to compare ESM-derived APO<sub>NCP</sub> directly to satellite-based APO<sub>NCP</sub> signals.  
3 | Extending model-derived insights to satellite products likely will require a shift in emphasis from  
4 | EP at an arbitrary reference depth to near-surface processes like NCP, which are more relevant  
5 | for exchanges of O<sub>2</sub> and CO<sub>2</sub> at the air-sea interface and more directly related to upward  
6 | radiances detected by satellites.

Cynthia Nevison 10/28/2014 12:05 PM

Formatted: Subscript

Cynthia Nevison 10/28/2014 12:05 PM

Formatted: Subscript

Cynthia Nevison 10/28/2014 11:58 AM

Deleted:

Cynthia Nevison 10/28/2014 12:06 PM

Deleted: may be more challenging and will

7 | ▼  
8 |  
9 | **Acknowledgements** The authors gratefully acknowledge the CMIP5 ocean modelers for  
10 | providing the output that made this project possible. In particular, we thank Keith Lindsay,  
11 | Laure Resplandy, and Cristoph Heinze for their assistance. We also thank Britt Stephens and an  
12 | anonymous reviewer for their helpful comments, which much improved the manuscript. Lastly,  
13 | we thank Michael Bender and Robert Mika for providing APO data and acknowledge support  
14 | from NASA Ocean Biology and Biogeochemistry grant NNX11AL73G.

Cynthia Nevison 10/24/2014 11:42 AM

Deleted: .

## 16 | **References**

17 | Anav, A., and Coauthors, 2013: Evaluating the Land and Ocean Components of the Global  
18 | Carbon Cycle in the CMIP5 Earth System Models. *J. Climate*, **26**, 6801–6843.  
19 | Arora, Vivek K., and Coauthors, 2013: Carbon–Concentration and Carbon–Climate Feedbacks in  
20 | CMIP5 Earth System Models. *J. Climate*, **26**, 5289–5314.  
21 | Aumont, O., E. Maier-Reimer, S. Blain, and P. Monfray (2003), An ecosystem model of the  
22 | global ocean including Fe, Si, P colimitations, *Global Biogeochem. Cycles*, 17, 1060,  
23 | doi:10.1029/2001GB001745

Cynthia Nevison 10/24/2014 11:42 AM

Deleted: . We

1 Aumont, O., and L. Bopp (2006), Globalizing results from ocean in situ iron fertilization studies,  
2 Global Biogeochem. Cycles, 20, GB2017, doi:10.1029/2005GB002591.

3 Battle, M., Mikaloff Fletcher, S., Bender, M.L., Keeling, R.F., Manning, A.C., Gruber, N., Tans,  
4 P.P., Hendricks, M.B., Ho, D.T., Simonds, C., Mika, R. and Paplawsky, B. (2006),  
5 Atmospheric potential oxygen: New observations and their implications for some  
6 atmospheric and oceanic models, Global Biogeochem. Cycles, 20, GB1010,  
7 doi:10.1029/2005GB002534, 2006.

8 Behrenfeld, M.J., and P.G. Falkowski (1997), Photosynthetic rates derived from satellite based  
9 chlorophyll concentration, *Limnol. Oceanogr.*, 42, 1-20.

10 Bender, M., Ho, D., Hendricks, M.B., Mika, R., Battle, M.O., Tans, P., Conway, T.J., Sturtevant,  
11 P. B., and Cassar, N. (2005), Atmospheric O<sub>2</sub>/N<sub>2</sub> changes, 1993-2002: Implications for  
12 the partitioning of fossil fuel CO<sub>2</sub> sequestration, Global Biogeochem. Cycles, 19,  
13 GB4017, doi:10.1029/2004GB002410.

14 Blaine, T., W. 2005. *Continuous Measurements of Atmospheric Ar/N<sub>2</sub> as a Tracer of Air-Sea*  
15 *Heat Flux: Models, Methods, and Data*. University of California, San Diego, La Jolla.

16 Bopp, L., Resplandy, L., Orr, J. C., Doney, S. C., Dunne, J. P., Gehlen, M., Halloran, P.,  
17 Heinze, C., Ilyina, T., Séférian, R., Tjiputra, J., and Vichi, M.: Multiple stressors of ocean  
18 ecosystems in the 21st century: projections with CMIP5 models, *Biogeosciences*, 10,  
19 6225-6245, doi:10.5194/bg-10-6225-2013, 2013.

20 Boyd, P. W. , S. C. Doney (2003) The impact of Climate Change and Feedback Processes on the  
21 Ocean Carbon Cycle. Chapter 7 , *Ocean Biogeochemistry, The role of the Ocean Carbon*  
22 *Cycle in Global Change*, Michael J. R. Fasham Editor, Springer-Verlag, pp. 157-198

1 Cadule, P., P. Friedlingstein, L. Bopp, S. Sitch, C. D. Jones, P. Ciais, S. L. Piao, and P. Peylin  
2 (2010), Benchmarking coupled climate-carbon models against long-term atmospheric  
3 CO<sub>2</sub> measurements, *Global Biogeochem. Cycles*, 24, GB2016,  
4 doi:10.1029/2009GB003556.

5 Dunne, J. P., R. A. Armstrong, A. Gnanadesikan, and J. L. Sarmiento (2005), Empirical and  
6 mechanistic models for the particle export ratio, *Global Biogeochem. Cycles*, 19,  
7 GB4026, doi:10.1029/2004GB002390.

8 Dunne, J. P., et al., 2012: GFDL's ESM2 global coupled climate-carbon Earth System Models  
9 Part I: Physical formulation and baseline simulation characteristics. *Journal of Climate*,  
10 doi:10.1175/JCLI-D-11-00560.1.

11 Dunne, J. P., et al., 2013: GFDL's ESM2 global coupled climate-carbon Earth System Models  
12 Part II: Carbon system formulation and baseline simulation characteristics. *Journal of*  
13 *Climate*, doi:10.1175/JCLI-D-12-00150.1.

14 Fay, A. R. and McKinley, G. A.: Global open-ocean biomes: mean and temporal variability,  
15 Earth Syst. Sci. Data, 6, 273-284, doi:10.5194/essd-6-273-2014, 2014.

16 Gruber, N., and Sarmiento, J. L. (2002), Large-scale biogeochemical-physical interactions in  
17 elemental cycles, in *The Sea*, Volume 12, Robinson, A.R., McCarthy, J.J. and Rothschild,  
18 B.J. (eds.), John Wiley & Sons, Inc., New York.

19 Gurney, K. R., R. Law, A.S. Denning, P. Rayner, D. Baker, P. Bousquet, L. Bruhwiler, Y.-H.  
20 Chen, P. Ciais, S. Fan, I. Fung, M. Gloor, M. Heimann, K. Higuchi, J. John, E.  
21 Kowalczyk, T. Maki, S. Maksyutov, P. Peylin, M. Prather, B. Pak, J. Sarmiento, S.  
22 Taguchi, T. Takahashi, C-W. Yuen (2003), Transcom 3 CO<sub>2</sub> inversion intercomparison:

Cynthia Nevison 10/27/2014 10:53 AM  
Formatted: Font:(Default) Times New Roman

Cynthia Nevison 10/27/2014 10:54 AM  
Formatted: Font:Times New Roman, 12 pt

1 [1. Annual mean control results and sensitivity to transport and prior flux information,](#)  
2 [Tellus, Ser. B, 55, 555–579.](#)

3 [Gurney, K. R., R. Law, A.S. Denning, P. Rayner, B. Pak, D. Baker, P. Bousquet, L. Bruhwiler,](#)  
4 [Y.-H. Chen, P. Ciais, S. Fan, I. Fung, M. Heimann, J. John, 2004, T. Maki, S.](#)  
5 [Maksyutov, P. Peylin, M. Prather, S. Taguchi, \(2004\), Transcom 3 inversion](#)  
6 [intercomparison: Model mean results for the estimation of seasonal carbon sources and](#)  
7 [sinks, Global Biogeochem. Cycles, 18, GB1010, doi:10.1029/2003GB002111.](#)

8 [Henson, S.A., Sarmiento, J.L., Dunne, J.P., Bopp, L., Lima, I., Doney, S.C., John, J., Beaulieu,](#)  
9 [C., 2010. Detection of anthropogenic climate change in satellite records of ocean](#)  
10 [chlorophyll and productivity. Biogeosciences 7, 621-640.](#)

11 [Henson, S. A., R. Sanders, E. Madsen, P. J. Morris, F. Le Moigne, and G. D. Quartly \(2011\), A](#)  
12 [reduced estimate of the strength of the ocean's biological carbon pump, Geophys. Res.](#)  
13 [Lett., 38, L04606, doi:10.1029/2011GL046735.](#)

14 [Henson, S., Cole, H., Beaulieu, C., and Yool, A.: The impact of global warming on seasonality](#)  
15 [of ocean primary production, Biogeosciences, 10, 4357-4369, doi:10.5194/bg-10-4357-](#)  
16 [2013, 2013.](#)

17 [Ilyina, T., K. D. Six, J. Segschneider, E. Maier-Reimer, H. Li, and I. N u~nez-Riboni \(2013\),](#)  
18 [Global ocean biogeochemistry model HAMOCC: Model architecture and performance as](#)  
19 [component of the MPI-Earth system model in different CMIP5 experimental realizations,](#)  
20 [J. Adv. Model. Earth Syst., 5, 287–315, doi:10.1029/2012MS000178.](#)

21 [Irwin, A. J. and M. J. Oliver \(2009\), Are ocean deserts getting larger ?, Geophys. Res. Lett., 36,](#)  
22 [L18609, doi:10.1029/2009GL039883](#)

Cynthia Nevison 10/27/2014 10:54 AM  
Formatted: Font:12 pt

Cynthia Nevison 10/27/2014 10:54 AM  
Formatted: Font:Times New Roman, 12 pt

Cynthia Nevison 10/27/2014 10:54 AM  
Formatted: Font:12 pt

Cynthia Nevison 10/27/2014 10:54 AM  
Formatted: Font:Times New Roman, 12 pt

Cynthia Nevison 10/27/2014 10:54 AM  
Formatted: Font:12 pt

Cynthia Nevison 10/21/2014 11:10 AM  
Deleted: .

1 Jiang, ChuanLi, Sarah T. Gille, Janet Sprintall, Colm Sweeney, 2014: Drake Passage Oceanic  
2 pCO<sub>2</sub>: Evaluating CMIP5 Coupled Carbon–Climate Models Using in situ Observations.  
3 *J. Climate*, **27**, 76–100.

4 Jin, X., Najjar, R.G., Louanchi, F., and Doney, S.C. (2007), A modeling study of the seasonal  
5 oxygen budget of the global ocean. *J. Geophys. Res.*, 112, C05017,  
6 doi:10.1029/2006JC003731.

7 Kahru, M., R. Kudela, M. Manzano-Sarabia and B.G. Mitchell (2009), Trends in primary  
8 production in the California Current detected with satellite data, *J. Geophys. Res.*, 114,  
9 C02004, doi:10.1029/2008JC004979.

10 Kahru, M. and B.G. Mitchell (2010), Blending of ocean colour algorithms applied to the  
11 Southern Ocean, *Remote Sensing Letters*, 1: 2, 119-124, doi:  
12 10.1080/01431160903547940.

13 Keeling, R. F., Najjar, R. P., Bender, M. L., and Tans, P. P. (1993), What atmospheric oxygen  
14 measurements can tell us about the global carbon cycle, *Global Biogeochem. Cycles*, 7,  
15 37–67.

16 Keeling, R.F., Stephens, B.B., Najjar, R.G., Doney, S.C., Archer, D., and Heimann, M. (1998),  
17 Seasonal variations in the atmospheric O<sub>2</sub>/N<sub>2</sub> ration in relation to the kinetics of air-sea  
18 gas exchange, *Global Biogeochem. Cycles*, 12, 141-163.

19 Keeling R. F. A. Koertzing, N Gruber (2010) Ocean Deoxygenation in warming world, *Annu.*  
20 *Mar. Rev. Sci*, 2:463-493.

21 Khatiwala, S., Primeau, F. and Hall, T. (2009) Reconstruction of the history of anthropogenic  
22 CO<sub>2</sub> concentrations in the ocean, *Nature*, 462, 346-350)

1 Laws, E. A., Falkowski, P. G., Smith, W. O., Jr., Ducklow, H. W., & McCarthy, J. J. 2000.  
2 Temperature effects on export production in the open ocean. *Global Biogeochemical*  
3 *Cycles*, 14(4): 1231-1246.

4 Laws, E. A. (2004), Export flux and stability as regulators of community composition in pelagic  
5 marine biological communities: Implications for regime shifts, *Progress in*  
6 *Oceanography*, 60(2-4), 343-353.

7 Lee, Z., et al. (2011), An assessment of optical properties and primary production derived from  
8 remote sensing in the Southern Ocean (SO GasEx), *J. Geophys. Res.*, 116, C00F03, doi:  
9 10.1029/2010JC006747.

10 [Lenton, A., B. Tilbrook, R. Law, D. Bakker, S. Doney, N. Gruber, M. Ishii, M. Hoppema, N.](#)  
11 [Lovenduski, R. Matear, B. McNeil, N. Metzl, S. Mikaloff Fletcher, P. Monteiro, C.](#)  
12 [Roedenbeck, C. Sweeney, T. Takahashi \(2013\), Sea-air CO<sub>2</sub> fluxes in the Southern](#)  
13 [Ocean for the period 1990-2009, Biogeosciences, 10, 4037-4054.](#)

14

15 Le Quéré, C., Roedenbeck, C., Buitenhuis ET, Conway TJ, Langenfelds R, et al. (2007),  
16 Saturation of the Southern Ocean CO<sub>2</sub> sink due to recent climate change. *Science* 316,  
17 1735-1738.

18 Maier-Reimer, E., Kriest, I., Segschneider, J., and Wetzel, P.: The HAMburg Ocean Carbon  
19 Cycle model HAMOCC5.1, Berichte zur Erdsystemforschung 14/2005, Max Planck-  
20 Institut für Meteorologie, Hamburg, Germany, 2005.

21 Manizza, M., R. F. Keeling, and C. D. Nevison, On the processes controlling the seasonal cycles  
22 of the air-sea fluxes of O<sub>2</sub> and N<sub>2</sub>O: A modeling study, *Tellus-B*, 64, 18429,  
23 <http://dx.doi.org/10.3402/tellusb.v64i0.18429>, 2012.

1 Manning, A. C. , R. F Keeling (2006) Global oceanic and land biotic carbon sinks from the  
2 Scripps atmospheric oxygen flask sampling network, *Tellus-B*, 58B, 95-116

3 Mitchell, B.G. (1992) Predictive bio-optical relationships for polar oceans and marginal ice  
4 zones. *J. of Marine Systems*, 3: 91-105.

5 Mitchell, B.G. and M. Kahru (2009), Bio-optical algorithms for ADEOS-2 GLI, *J. Remote*  
6 *Sensing Soc. of Japan*, 29, 1, 80-85.

7 Moore, J.K., Doney, S.C., Kleypas, J.C., Glover, D.M., Fung, I.Y., (2002) An intermediate  
8 complexity marine ecosystem model for the global domain, *Deep-Sea Res. II*, 49: 403-  
9 462.

10 Moore, J.K., Doney, S.C., and Lindsay, K. (2004) Upper ocean ecosystem dynamics and iron  
11 cycling in a global 3D model, *Global Biogeochem. Cycles*, 18, GB4028,  
12 doi:10.1029/2004GB002220

13 Moore, J., K. Lindsay, S. Doney, M. Long, and K. Misumi, 2013: Marine Ecosystem Dynamics  
14 and Biogeochemical Cycling in the Community Earth System Model [CESM1(BGC)]:  
15 Comparison of the 1990s with the 2090s under the RCP4.5 and RCP8.5 Scenarios. *J.*  
16 *Climate*, 26, 9291-9312, doi:10.1175/JCLI-D-12-00566.1.

17 Naegler T, P. Ciais, J. Orr, O. Aumont, C. Roedenbeck (2007) On evaluating ocean models with  
18 atmospheric potential oxygen, *Tellus*, Vol 59B, 138-156.

19 Najjar, R.G., et al. (2007) Impact of circulation on export production, dissolved organic matter,  
20 and dissolved oxygen in the ocean: Results from Phase II of the Ocean Carbon-cycle  
21 Model Intercomparison Project (OCMIP-2), *Global Biogeochem. Cycles*, 21, GB3007,  
22 doi:10.12007.

1 Nevison, C.D., R.F. Keeling, R.F. Weiss, B.N. Popp, X. Jin, P.J. Fraser, L.W. Porter and P.G.  
2 Hess (2005), Southern Ocean ventilation inferred from seasonal cycles of atmospheric  
3 N<sub>2</sub>O and O<sub>2</sub>/N<sub>2</sub> at Cape Grim, Tasmania, *Tellus*, 57B, 218-229.

4 Nevison, C. D., Mahowald, N. M., Doney, S. C., Lima, I. D., and Cassar, N.: Impact of variable  
5 air-sea O<sub>2</sub> and CO<sub>2</sub> fluxes on atmospheric potential oxygen (APO) and land-ocean carbon  
6 sink partitioning, *Biogeosciences*, 5, 875-889, 2008.

7 Nevison, C.D. E. Dlugokencky, G. Dutton, J.W. Elkins, P. Fraser, B. Hall, P.B. Krummel, R.L.  
8 Langenfelds, S. O'Doherty, R.G. Prinn, L.P. Steele, R.F. Weiss, Exploring causes of  
9 interannual variability in the seasonal cycles of tropospheric nitrous oxide, *Atmospheric*  
10 *Chemistry and Physics*, 11, doi:10.5194/acp-11-1-2011, 1-18, 2011.

11 Nevison, C. D., R. F. Keeling, M. Kahru, M. Manizza, B. G. Mitchell, and N. Cassar, Estimating  
12 net community production in the Southern Ocean based on atmospheric potential oxygen  
13 and satellite ocean color data, *Global Biogeochem. Cycles*, 26, GB1020,  
14 doi:10.1029/2011GB004040, 2012.

15 Nevison, C.D., D.F. Baker, and K.R. Gurney, A methodology for estimating seasonal cycles of  
16 atmospheric CO<sub>2</sub> resulting from terrestrial net ecosystem exchange (NEE) fluxes using  
17 the Transcom T3L2 pulse-response functions, *Geosci. Model Dev. Discuss.*, 5, 2789-  
18 2809, 2012, [www.geosci-model-dev-discuss.net/5/2789/2012/](http://www.geosci-model-dev-discuss.net/5/2789/2012/) doi:10.5194/gmdd-5-2789-  
19 2012, 2012b.

20 [Peylin, P., R. Law, K. Gurney, F. Chevalier, A. Jacobson, T. Maki, Y. Niwa, P. Patra, W. Peters,](#)  
21 [P. Rayner, C. Roedenbeck, J. van der Laan-Luijkx, X. Zhang \(2013\), Global atmospheric](#)  
22 [carbon budget: results from an ensemble of atmospheric CO<sub>2</sub> inversions, \*Biogeosciences\*,](#)  
23 [10, 6699-6720.](#)

Cynthia Nevison 10/23/2014 2:33 PM  
Formatted: Subscript

1 Polovina, J. J., E. A. Howell, and M. Abecassis (2008), Ocean's least productive waters are  
2 expanding, *Geophys. Res. Lett.*, 35, L03618, doi:10.1029/2007GL031745.

3 Roy, T., et al., 2011: Regional Impacts of Climate Change and Atmospheric CO<sub>2</sub> on Future  
4 Ocean Carbon Uptake: A Multimodel Linear Feedback Analysis. *Journal of Climate*, **24**,  
5 2300-2318.

6 Sauer, M.J., Roesler, C.S., Werdell, J.P., Barnard, A., 2012. Under the hood of satellite empirical  
7 chlorophyll algorithms: revealing the dependencies of maximum band ratio algorithms on  
8 inherent optical properties, *Optics Express* 20, 20920-20933.

9 Schneider B., L. Bopp, M. Gehlen, J. Segschneider, T. L. Frölicher, P. Cadule, P. Friedlingstein,  
10 S. C. Doney, M. J. Behrenfeld, and F. Joos (2008) Climate-induced interannual  
11 variability of marine primary and export production in three global coupled climate  
12 carbon cycle models, *Biogeosciences*, 5, 597-614.

13 Siegel, D. A., S. Maritorena, N. B. Nelson, and M. J. Behrenfeld (2005), Independence and  
14 interdependencies among global ocean color properties: Reassessing the bio-optical  
15 assumption, *J. Geophys. Res.*, 110, C07011, doi:10.1029/2004JC002527.

16 Sigman, D.M., M.P. Hain, G.H. Haug, The polar ocean and glacial cycles in atmospheric CO<sub>2</sub>,  
17 *Nature* 466, 47-55, 2010.

18 Six, K. and Maier-Reimer, E.: Effects of plankton dynamics on seasonal carbon fluxes in an  
19 ocean general circulation model, *Global Biogeochem Cy.*, 10, 559–583, 1996.

20 Steinacher, M., F. Joos, T.L. Frölicher, L. Bopp, P. Cadule, V. Cocco, S.C. Doney, M. Gehlen,  
21 K. Lindsay, J.K. Moore, B. Schneider and J. Segschneider, Projected 21<sup>st</sup> century  
22 decrease in marine productivity: a multi-model analysis, *Biogeosciences*, 7, 979-1005,  
23 2010.

1 Stephens, B.B., Keeling, R.F., Heimann, M., Six, K.D., Murnane, R. and Caldeira, K. (1998),  
 2 Testing global ocean carbon cycle models using measurements of atmospheric O<sub>2</sub> and  
 3 CO<sub>2</sub> concentration, *Global Biogeochem. Cycles*, 12, 213-230.

4 Stephens, B.B., et al. (2007), Weak northern and strong tropical land carbon uptake from vertical  
 5 profiles of atmospheric CO<sub>2</sub>, *Science*, 316, 1732-1735, doi: 10.1126/science.1137004.

6 Tjiputra, J.F., C. Roelandt, M. Bentsen, D.M. Lawrence, T. Lorentzen, J. Schwinger, Ø. Seland,  
 7 and C. Heinze, Evaluation of the carbon cycle components in the Norwegian Earth  
 8 System Model (NorESM), *Geosci. Model Dev.*, 6, 301-325, 2013

9 Tohjima, Y., H. Mukai, T. Machida, Y. Nojiri, and M. Gloor (2005), First measurements of the  
 10 latitudinal atmospheric O<sub>2</sub> and CO<sub>2</sub> distributions across the western Pacific, *Geophys.*  
 11 *Res. Lett.*, 32, L17805, doi:10.1029/2005GL023311.

12 Tohjima, Y., C. Minejima, H. Mukai, T. Machida, H. Yamagishi, and Y. Nojiri (2012), Analysis  
 13 of seasonality and annual mean distribution of atmospheric potential oxygen (APO) in the  
 14 Pacific region, *Global Biogeochem. Cycles*, 26, GB004110, doi:10.1029/2011GB004110.

15 Uitz, J., H. Claustre, B. Gentili, and D. Stramski (2010), Phytoplankton class-specific primary  
 16 production in the world's oceans: Seasonal and interannual variability from satellite  
 17 observations, *Global Biogeochem. Cycles*, 24, GB3016, doi:10.1029/2009GB003680

18 Vancoppenolle, M., L. Bopp, G. Madec, J. Dunne, T. Ilyina, P. R. Halloran, and N. Steiner  
 19 (2013), Future Arctic Ocean primary productivity from CMIP5 simulations: Uncertain  
 20 outcome, but consistent mechanisms, *Global Biogeochem. Cycles*, 27, 605–619,  
 21 doi:10.1002/gbc.20055.

22 Wofsy, S. C., the HIPPO Science Team and Cooperating Modellers and Satellite Teams:  
 23 HIAPER Pole-to-Pole Observations (HIPPO): Fine grained, global scale measurements

Cynthia Nevison 10/21/2014 1:28 PM  
 Formatted: Font:(Default) Times New Roman, 12 pt

Cynthia Nevison 10/23/2014 2:44 PM  
 Formatted: Font:Times New Roman, 12 pt

Cynthia Nevison 10/23/2014 2:44 PM  
 Formatted: Font:12 pt

Cynthia Nevison 10/23/2014 2:44 PM  
 Formatted: Font:Times New Roman, 12 pt

1 [for determining rates for transport, surface emissions, and removal of climatically](#)  
2 [important atmospheric gases and aerosols, Phil. Trans. of the Royal Society A,](#)  
3 [369\(1943\), doi:10.1098/rsta.2010.0313, 2073-2086, 2011.](#)  
4  
5  
6  
7  
8  
9  
10

**Table 1:** Vertically integrated NPP, EP at 100m (both in PgC yr-1) and EP/PP (ef-ratio) for 6 CMIP5 models and 2 Satellite Products.

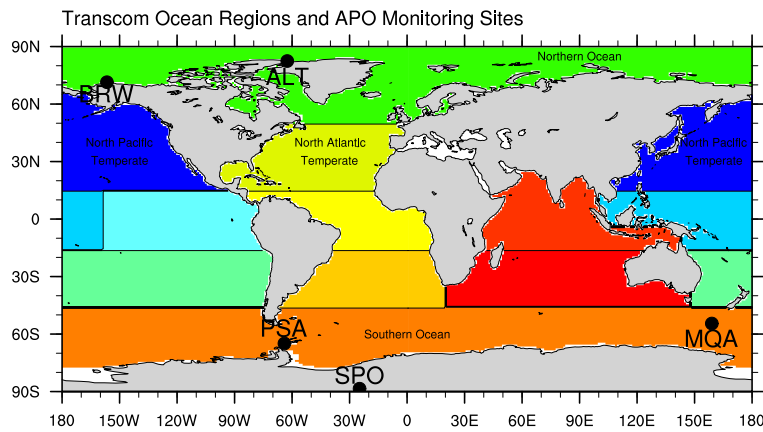
Model	CESM	ESM2M	ESM2G	IPSL	NorESM1	MPIM	VGPM	SPGANT*
<b>Global</b>								
EP	7.97	7.78	5.27	7.02	8.00	8.26	8.20	N/A
NPP	56.3	82.2	66.5	33.6	41.0	57.9	45.42	N/A
EP/NPP	0.14	0.095	0.08	0.21	0.20	0.14	0.18	N/A
<b>40-60N</b>								
EP	0.71	0.83	0.53	0.75	0.66	0.51	1.47	N/A
NPP	3.85	4.71	3.92	2.42	3.45	3.77	4.97	N/A
EP/NPP	0.19	0.18	0.14	0.31	0.19	0.13	0.30	N/A
<b>60-90N</b>								
EP	0.34	0.33	0.21	0.19	0.15	0.08	0.46	N/A
NPP	1.48	1.35	0.95	0.58	0.74	0.75	1.29	N/A
EP/NPP	0.23	0.24	0.22	0.33	0.20	0.11	0.36	N/A
<b>40-60S</b>								
EP	1.25	1.18	0.82	1.42	1.93	1.77	1.60	2.85
NPP	6.77	9.36	8.53	5.24	10.3	12.5	6.01	8.81
EP/NPP	0.18	0.13	0.10	0.27	0.19	0.14	0.27	0.32

\* SPGANT totals are only shown for the 40-60°S band because the algorithm is optimized for the Southern Ocean but not well validated in the Northern Hemisphere.

1

2

### 3 Figures



Unknown

Formatted: Font:Times New Roman, 12 pt

4

5 Figure 1. Transcom3 Level 2 ocean regions used in the matrix-based atmospheric transport  
6 method. Locations of the 5 APO monitoring sites featured in Figure 2 are superimposed.

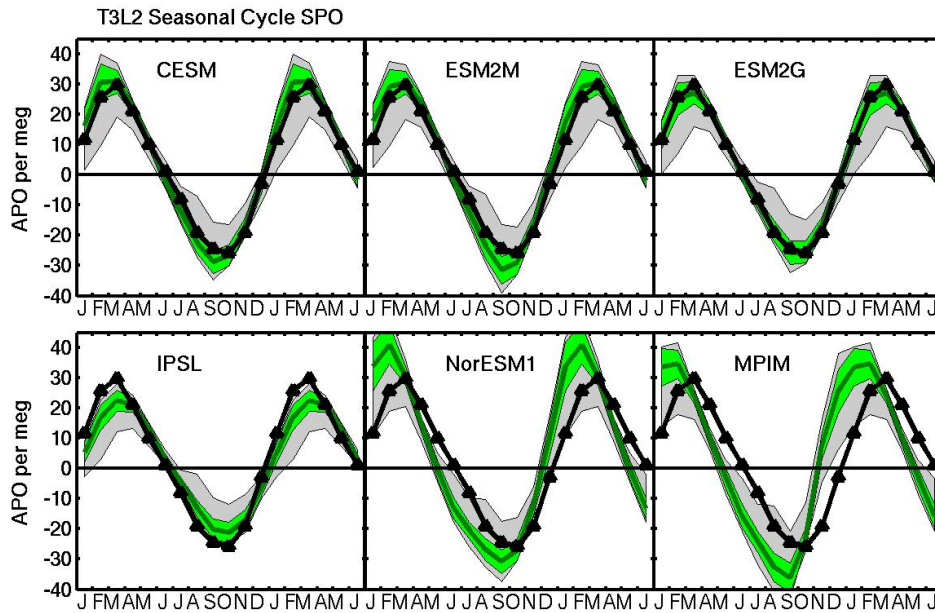
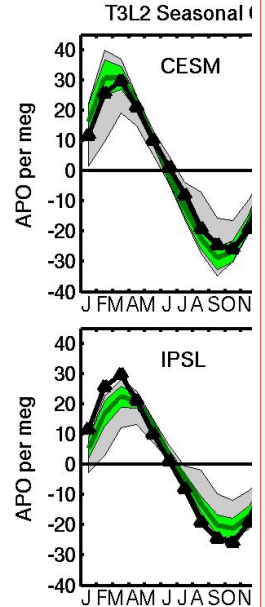


Figure 2. Results of the pulse-response code forced by  $O_2$ ,  $N_2$  and  $CO_2$  air-sea fluxes from 6 ESM ocean biogeochemistry model components. The dark green line and light green window show the mean and standard deviation, respectively, of the 9 ATMs participating in both T3L2 and APO Transcom. The amplitudes are scaled for each ATM and monitoring site based on the validation exercise described in Section 2.2.2 and illustrated in the Supplementary Material. The gray window shows the full range of responses from all 13 T3L2 ATMs, uncorrected based on the APO Transcom validation exercise. The heavy black line shows the observed APO mean annual cycle. a) Results at South Pole, compared to SIO observations.

Cynthia Nevison 10/23/2014 6:20 PM



Deleted:

Unknown

Formatted: Font:Times New Roman, 12 pt

Cynthia Nevison 10/27/2014 2:19 PM

Deleted: I

Cynthia Nevison 10/23/2014 4:10 PM

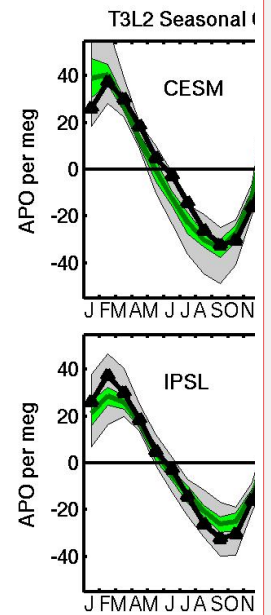
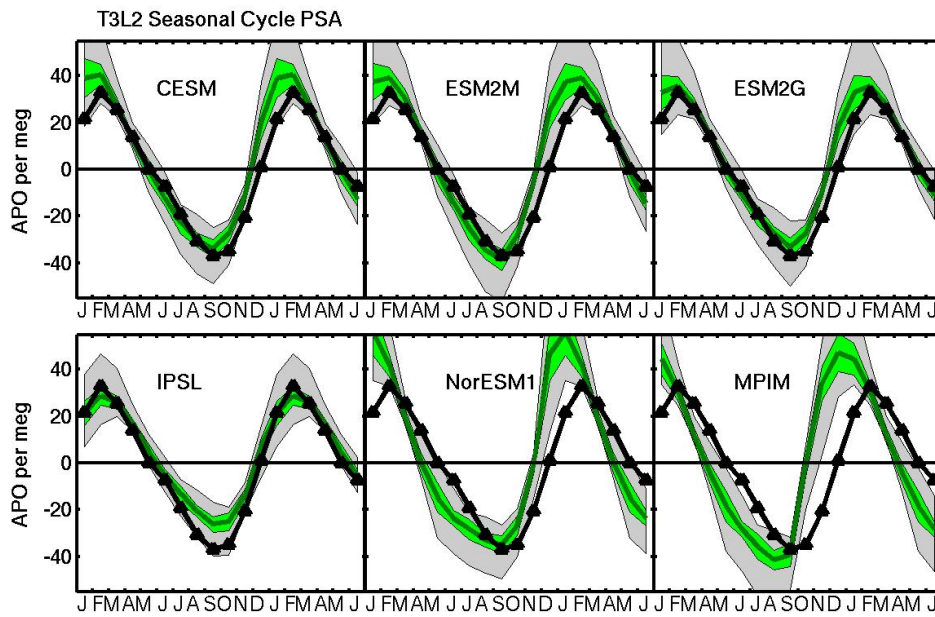
Deleted: APO

Cynthia Nevison 10/24/2014 12:13 PM

Deleted:

Cynthia Nevison 10/23/2014 4:12 PM

Deleted: y



Cynthia Nevison 10/23/2014 6:21 PM

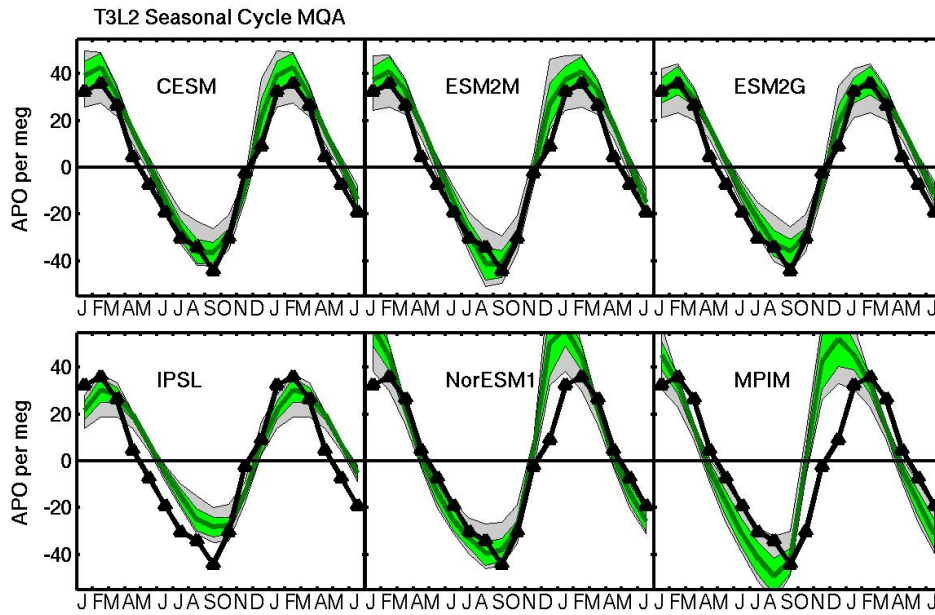
Deleted:

Unknown

Formatted: Font:Times New Roman, 12 pt, Bold

Cynthia Nevison 10/27/2014 2:20 PM

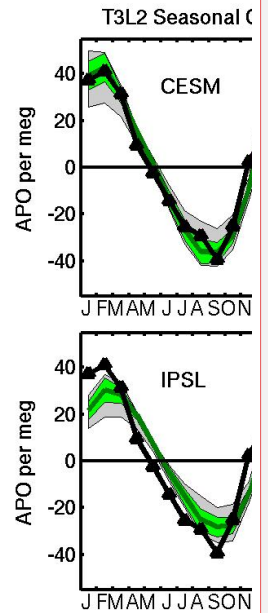
Deleted: 1



1

2 [2c](#)) Results at Macquarie Island (54.5°S, 159°E), compared to PU observations.

Cynthia Nevison 10/23/2014 6:22 PM



Deleted:

Unknown

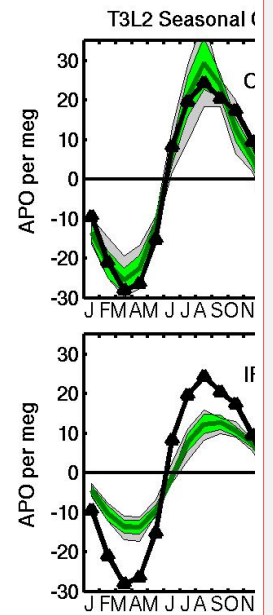
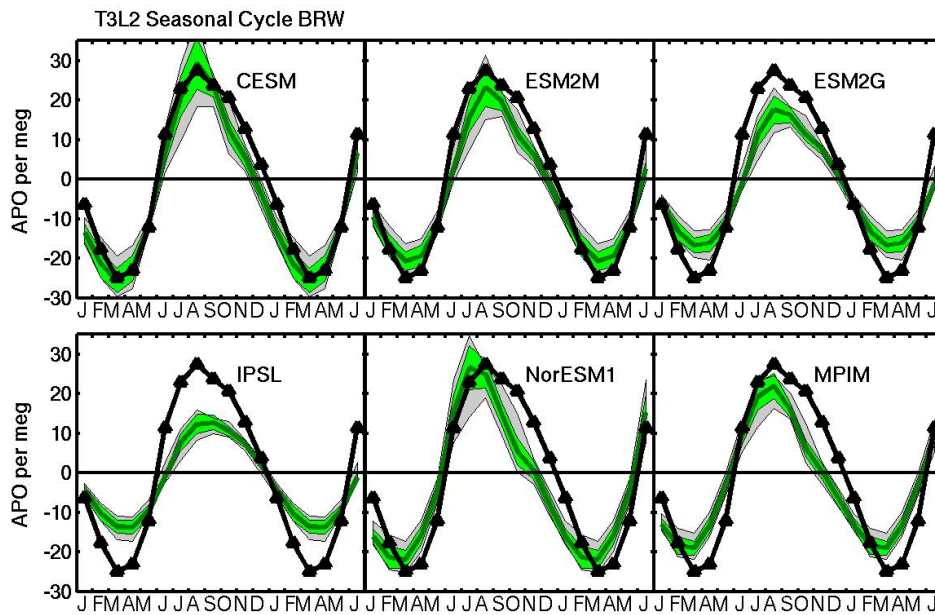
Formatted: Font:Times New Roman, 12 pt, Bold

Cynthia Nevison 10/27/2014 2:20 PM

Deleted: I

Cynthia Nevison 10/23/2014 4:13 PM

Deleted: )



2d) Results at Barrow, Alaska (71.3°N, 156.6°W), compared to PU observations,

Cynthia Nevison 10/23/2014 6:22 PM

Deleted:

Unknown

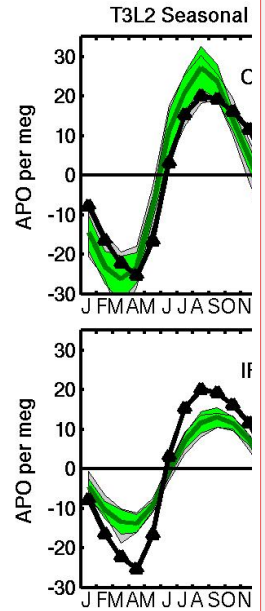
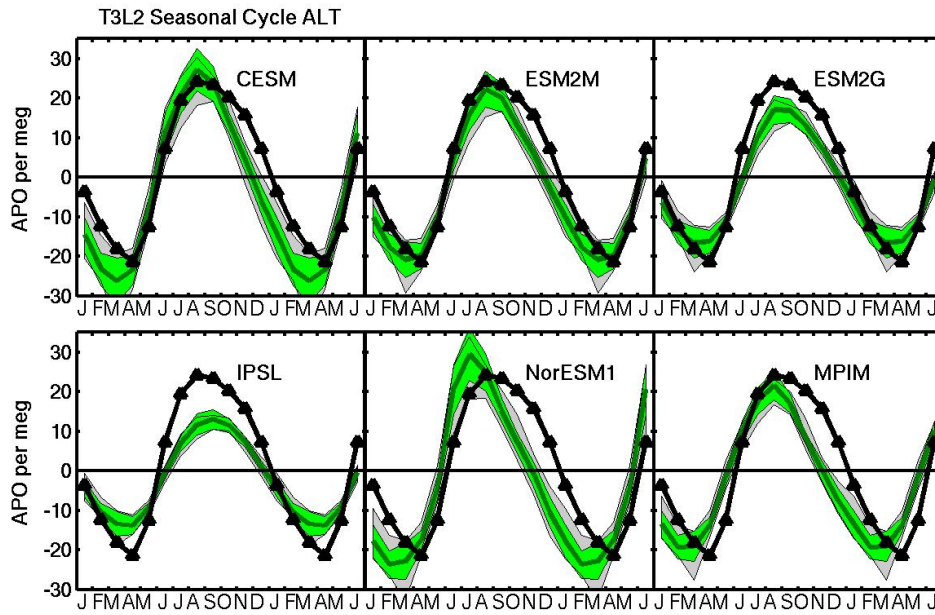
Formatted: Font:Times New Roman, 12 pt

Cynthia Nevison 10/27/2014 2:20 PM

Deleted: I

Cynthia Nevison 10/23/2014 4:13 PM

Deleted: )



2e) Results at Alert, Canada (82.5°N, 62.5°W), compared to SIO observations.

Deleted:

Unknown

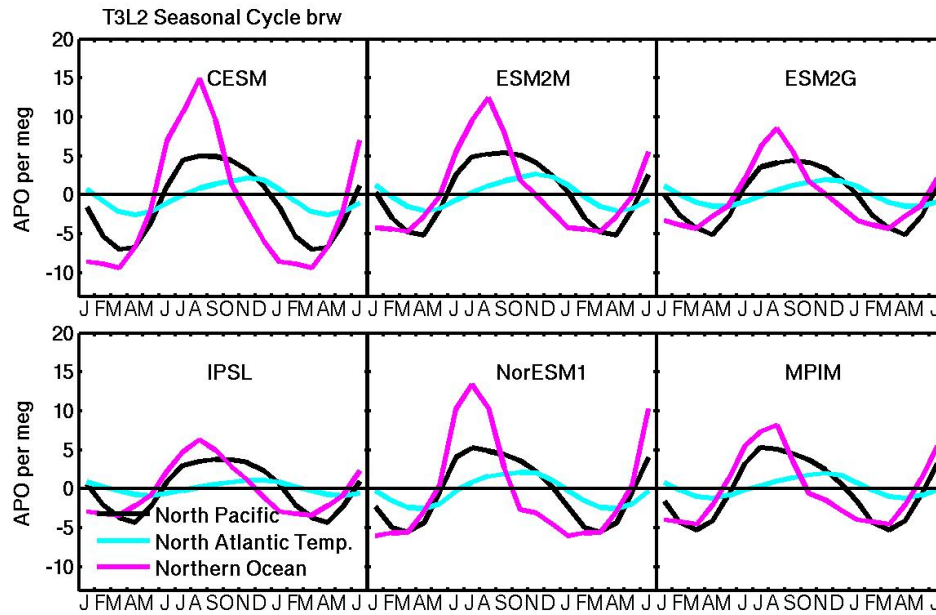
Formatted: Font:Times New Roman, 12 pt, Bold

Cynthia Nevison 10/27/2014 2:20 PM

Deleted: I

Cynthia Nevison 10/23/2014 4:13 PM

Deleted: )



1

2

3

4

5

Figure 3. Partitioning the APO cycle at Barrow, Alaska into its main regional contributions, North Pacific (black), Temperate North Atlantic (cyan) and Northern Ocean (magenta), which includes the North Atlantic north of 48N and the Arctic Ocean. All curves reflect the unscaled model mean of the 13 ATMs used in the matrix method.

Cynthia Nevison 10/27/2014 2:18 PM

Deleted: 2

Cynthia Nevison 10/23/2014 6:29 PM

Deleted: red

Cynthia Nevison 10/23/2014 6:29 PM

Deleted: green

Cynthia Nevison 10/23/2014 6:29 PM

Deleted: blue

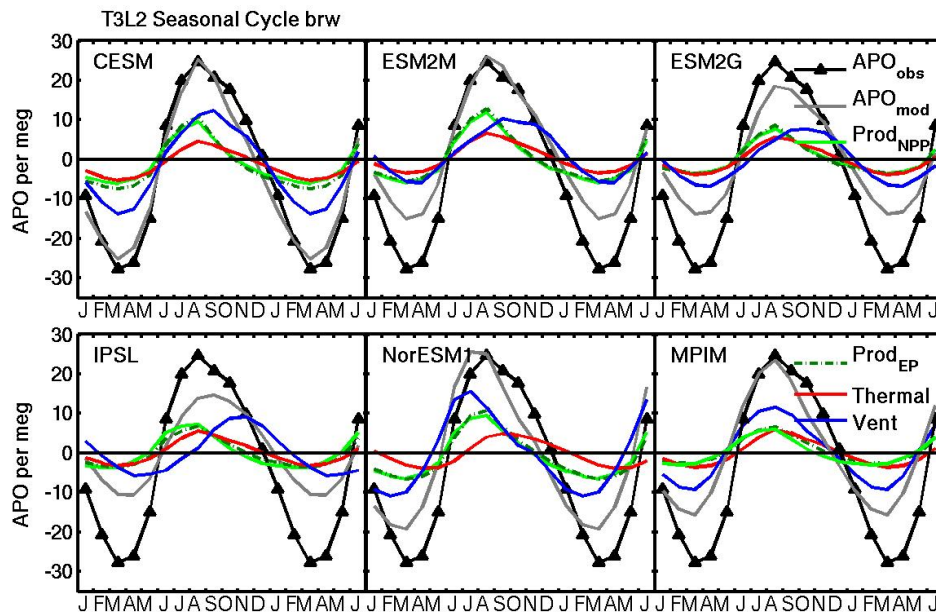


Figure 4. Partitioning of the model mean APO cycle into NCP, thermal and residual ventilation components at Barrow, Alaska. The  $APONCP$  components are estimated alternatively based on ocean model EP at 100m ( $Prod_{EP}$  light green, solid curve) and vertically-integrated NPP ( $Prod_{NPP}$ ) scaled by the mean ratio of  $EP_{100}/NPP$  (f ratio) between 40–60°N of the given ocean model (dark green, dashed curve). All components were translated into atmospheric signals as described in section 2.2.3. Also shown is  $APO_{vent}$  (blue), calculated as a residual of  $APONCP - APO_{therm}$ . With the exception of observed APO, all curves reflect the unscaled mean of the 13 ATMs used in the matrix method.

Unknown  
Formatted: Font:Times New Roman

Cynthia Nevison 10/23/2014 11:16 AM  
Deleted:

Cynthia Nevison 10/27/2014 2:18 PM  
Deleted: 3

Cynthia Nevison 10/23/2014 11:17 AM  
Deleted: and

Unknown  
Formatted: Font:Times New Roman

Cynthia Nevison 10/23/2014 11:21 AM  
Deleted:

Cynthia Nevison 10/23/2014 11:20 AM  
Deleted: have been

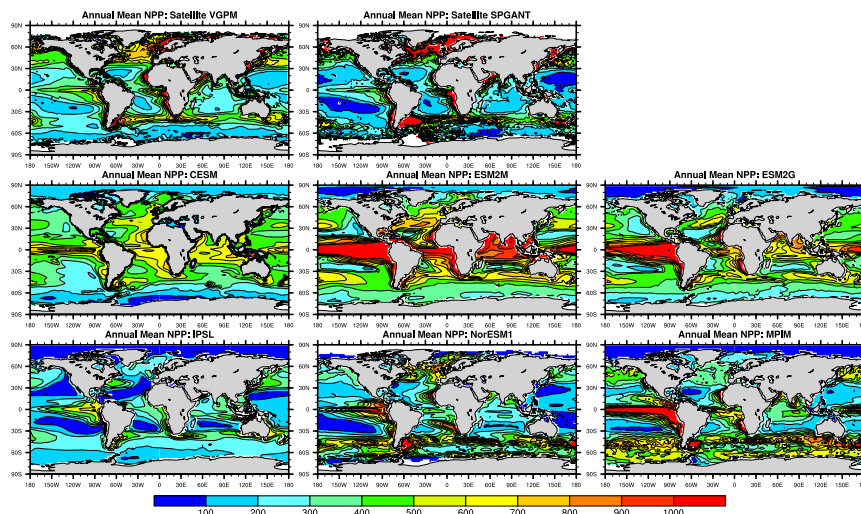
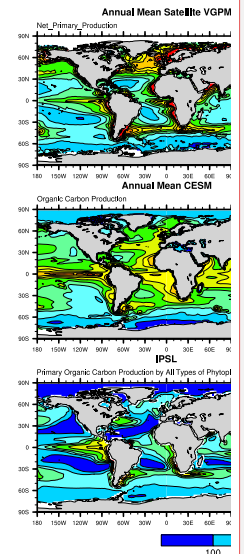


Figure 5. Annual mean NPP (in  $\text{mg C m}^{-2} \text{ day}^{-1}$ ). Top row: MODIS-Aqua data input to the VGPM NPP model and b) SeaWiFS data input to the SPGANT algorithm as described in Nevison *et al.* [2012]. Rows 2 and 3 show the corresponding NPP fields from 6 ESMs for the mean of 1997-2005.



Deleted:

Unknown

Formatted: Font:Times New Roman, 12 pt

Cynthia Nevison 10/27/2014 2:17 PM

Deleted: 4

Cynthia Nevison 10/23/2014 6:32 PM

Deleted: using top row)

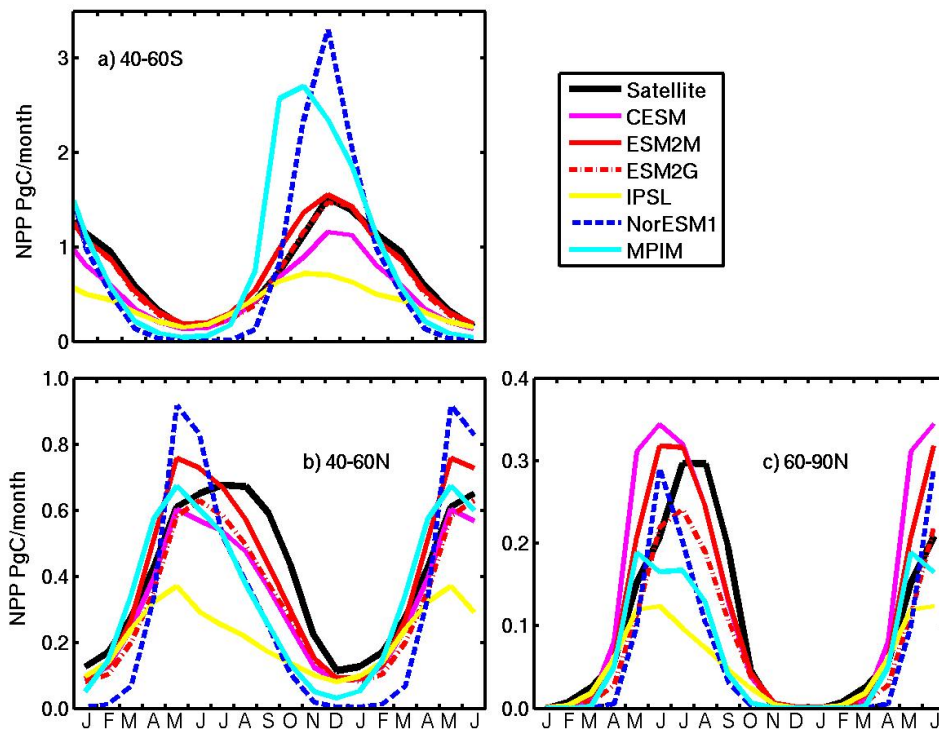


Figure 6. Comparison of the NPP (PgC month) mean annual cycle as simulated by ESMs and satellite-derived observations integrated over: a) 40-60°S, b) 40-60°N, c) 60-90°N. The satellite data are from SPGANT/Laws in panel (a) and VGPM/Dunne in panels (b-c).

Cynthia Nevison 10/27/2014 2:16 PM

Deleted: 5

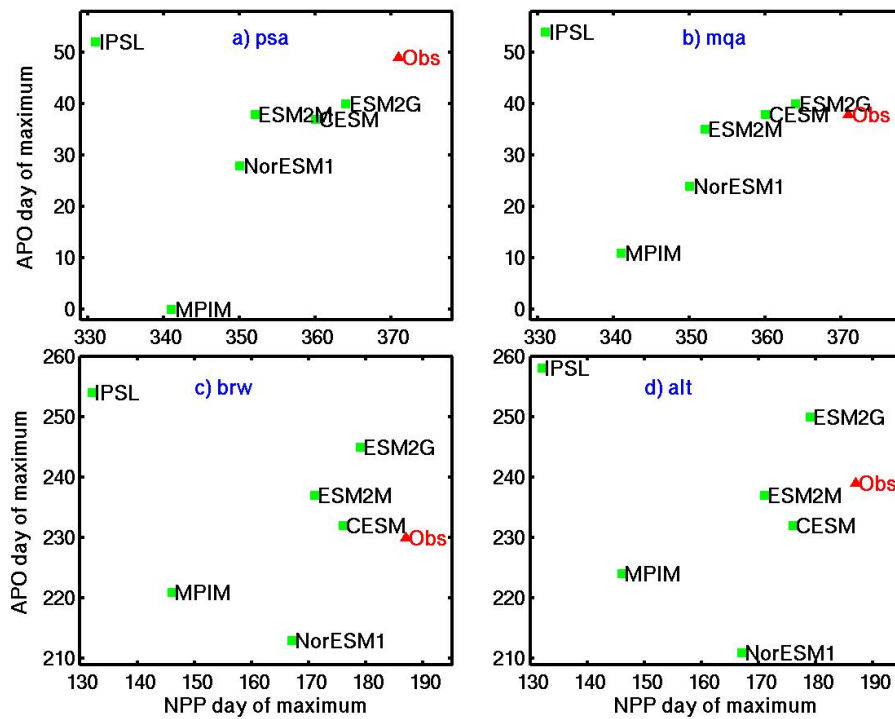
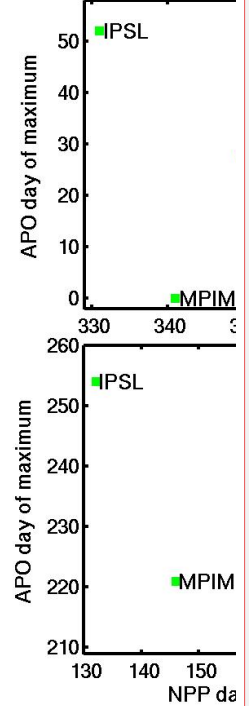


Figure 7. Day of APO maximum, plotted against day of NPP maximum. The observed data point is derived from APO data at a) Palmer Station, b) Macquarie, c) Barrow and d) Alert plotted against satellite NPP data integrated over the 40-60 degree latitude band of the appropriate hemisphere.

Cynthia Nevison 10/23/2014 6:47 PM



Deleted:

Unknown

Formatted: Font:Times New Roman, 12 pt

Cynthia Nevison 10/27/2014 2:15 PM

Deleted: 6

Cynthia Nevison 10/23/2014 6:38 PM

Deleted: maximum of total

Cynthia Nevison 10/23/2014 6:38 PM

Deleted: total

Cynthia Nevison 10/23/2014 6:38 PM

Deleted: maximum of

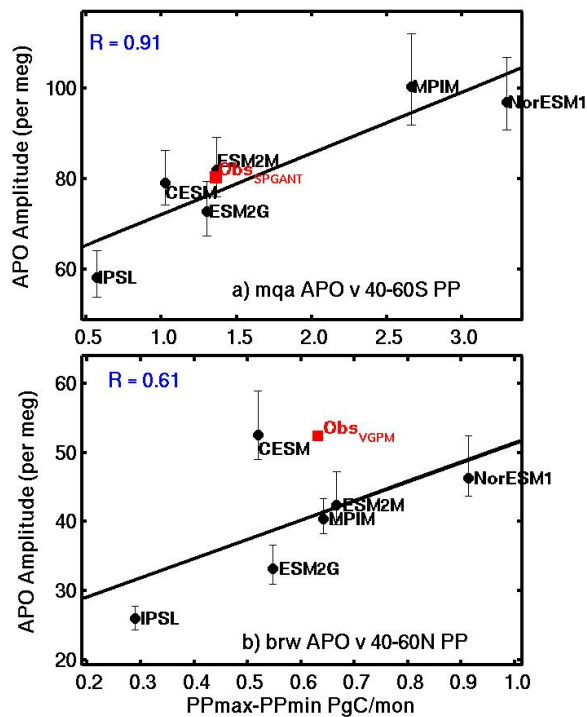
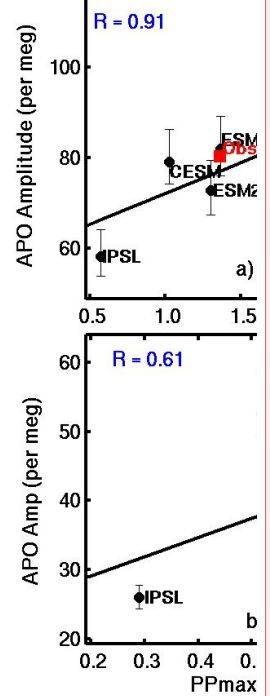


Figure 8a. Seasonal amplitude in APO at Macquarie Island (MQA), located at 54.5S, 159E, as estimated from the air-sea  $O_2$ ,  $CO_2$  and heat fluxes from 6 ESMs, plotted against the seasonal amplitude of  $\downarrow NPP$  integrated from 40-60S. Error bars represent the ATM uncertainty in model APO as estimated with the matrix method. The “Observed” data points (in red) are based on APO data from the [PU](#) network at Macquarie and NPP from the SPGANT satellite ocean color algorithms, as described in the text. The correlation coefficient  $R$  refers to regression through ESM points only, b) Same as 8a, but plotting seasonal amplitude in APO at Barrow, Alaska against the seasonal amplitude of  $\downarrow NPP$  integrated from 40-60N. The “Observed” data point is based on APO data from the [PU](#) network and the VGPM algorithm with MODIS-Aqua input.



Deleted:

Unknown

Formatted: Font:Times New Roman, 12 pt

Cynthia Nevison 10/27/2014 2:14 PM

Deleted: 7

Cynthia Nevison 10/23/2014 6:58 PM

Deleted: model

Cynthia Nevison 10/23/2014 9:20 PM

Deleted: Princeton

Cynthia Nevison 10/23/2014 6:59 PM

Deleted: C

Cynthia Nevison 10/23/2014 6:58 PM

Deleted: slope

Cynthia Nevison 10/27/2014 2:14 PM

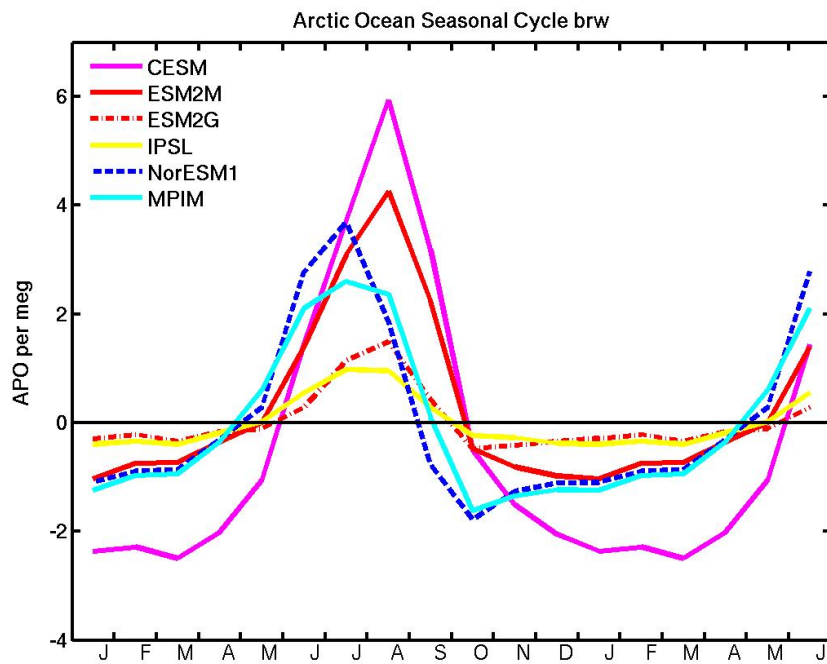
Deleted: 7

Cynthia Nevison 10/23/2014 6:58 PM

Deleted: model

Cynthia Nevison 10/23/2014 9:21 PM

Deleted: SIO



1  
2 | Figure 9. APO cycle at Barrow, Alaska from the Transcom Northern Ocean region, restricted to  
3 latitudes north of 65°N to estimate the contribution of the Arctic Ocean. All curves reflect the  
4 unscaled model mean of 13 ATMs used in the matrix method.

Cynthia Nevison 10/27/2014 2:13 PM  
Deleted: 8

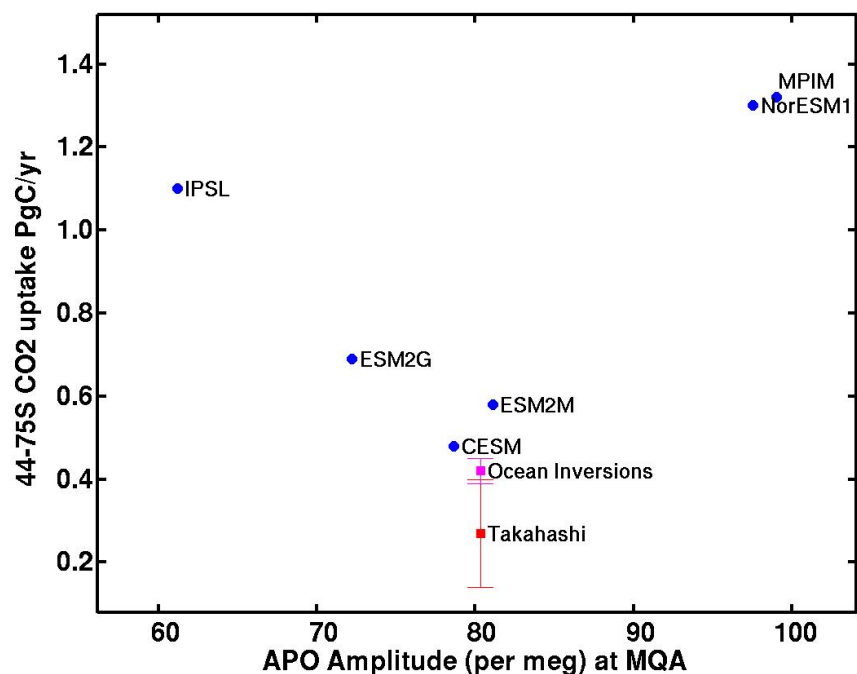
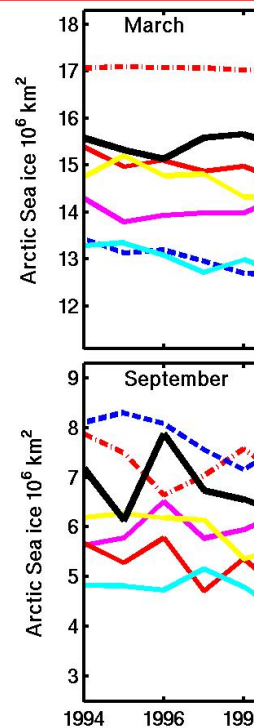


Figure 10. Annual mean CO<sub>2</sub> uptake in the Southern Ocean for 1997-2005 integrated 44-75°S plotted vs. mean APO amplitude at Macquarie over the same period, as predicted by 6 ESMs. Independent estimates of carbon uptake from ocean inversions and observed pCO<sub>2</sub> databases [Lenton et al., 2013], plotted against the observed APO amplitude at Macquarie are shown for reference.



Deleted:  
Cynthia Nevison 10/27/2014 2:11 PM  
Deleted: 9  
Unknown  
Formatted: Font:Times New Roman, 12 pt  
Cynthia Nevison 10/24/2014 10:06 AM  
Formatted: Subscript  
Cynthia Nevison 10/24/2014 9:38 AM  
Deleted: Changes in total Arctic sea ice cover in 10<sup>6</sup> km<sup>2</sup> predicted over 1994-2005 compared to observed values from the National Snow and Ice Data Center. a) March, b) September.

## Evaluating the ocean biogeochemical components of earth system models using atmospheric potential oxygen (APO) and ocean color data

### Supplemental Material

This section presents an evaluation of the 9 ATMs participating in both the T3L2 and APO Transcom experiments. The seasonal cycle in atmospheric potential oxygen (APO) at a variety of northern and southern monitoring sites is estimated using the pulse-response code (PRC) described in the main text and from APO Transcom forward simulations (FS) described below. All simulations are forced by monthly mean air-sea O<sub>2</sub> and N<sub>2</sub> fluxes from the climatology of Garcia and Keeling [2001].

In contrast to the matrix-based PRC simulations, which used uniform regional distributions of O<sub>2</sub> and N<sub>2</sub>, the archived APO Transcom forward simulations were forced by fine-scale (0.5 x 0.5 degree) monthly mean air-sea flux distributions (interpolated by APO Transcom from the original 1.125 degree resolution of Garcia and Keeling [2001]). The simulations were run by each participating model group with the fluxes turned on for the first year and turned off for the last two years. The resulting ATM atmospheric O<sub>2</sub> and N<sub>2</sub> fields in ppm were sampled in each of the 36 months of the simulations at 253 monitoring sites. The steady-state response, i.e., the mean seasonal cycle, was computed by summing all Januaries, Februaries, etc., for the three years. Conceptually, this calculation assumes that the ATM behaves linearly and that the steady-state response can be represented as the sum of the response to the fluxes from the present year, the past year, and two years previously, which correspond to the first, second, and third years of the simulations, respectively.

In using the archived APO Transcom results, it was necessary to account for several irregularities. First, the JMA O<sub>2</sub> and N<sub>2</sub> results were multiplied by 10<sup>6</sup> to convert to ppm units. Second, TM3 ran all 36 months with pulses on, so instead of summing all 3 sets of Januaries, Februaries, etc., the mean annual cycle was calculated based on the third year of the simulation alone. Finally, GISS UCI in principle was a 10<sup>th</sup> model that participated in both T3L2 and APO Transcom, but in practice it could not be used because only the first (pulse-on) year of GISS UCI output was submitted to APO Transcom.

Cynthia Nevison 10/24/2014 1:09 PM

Deleted: E

Cynthia Nevison 10/24/2014 1:10 PM

Deleted: , in which t

Cynthia Nevison 10/24/2014 1:10 PM

Deleted: above

Cynthia Nevison 10/24/2014 12:57 PM

Formatted: Subscript

Cynthia Nevison 10/24/2014 12:57 PM

Formatted: Subscript

Cynthia Nevison 10/24/2014 1:11 PM

Formatted: Font:Italic

Cynthia Nevison 10/24/2014 12:58 PM

Formatted: Subscript

Cynthia Nevison 10/24/2014 1:00 PM

Formatted: Subscript

Cynthia Nevison 10/24/2014 1:00 PM

Formatted: Subscript

Cynthia Nevison 10/24/2014 1:01 PM

Formatted: Superscript

Cynthia Nevison 10/24/2014 1:03 PM

Formatted: Superscript

**Table S1.** Mean values of the correlation coefficient  $R$  and the ratio of standard deviations:  $\sigma_{\text{pre}}/\sigma_{\text{fs}}$ , representing the PRC vs. FS correlation in the shape and phase and the amplitude ratio, respectively, of the seasonal cycle in APO among 6 extratropical monitoring sites in the Southern Hemisphere (SPO, SYO, PSA, MQA, CGO, AMS) and 6 extratropical sites in the Northern Hemisphere (LJO, RYO, SBL, CBA, BRW, ALT) – see also Figure S1. For  $\sigma_{\text{pre}}/\sigma_{\text{fs}}$ , the standard deviation among ratios at individual stations (in parentheses) is given.

ATM	Correlation Coefficient $R^2$		$\sigma_{\text{pre}}/\sigma_{\text{fs}}$	
	>25°N	≤ -25°S	>25°N	≤ -25°S
GCTM	0.9 <del>5</del>	0.9 <del>8</del>	0.8 <del>6</del> (0.21)	0.91 (0.10)
GISS:UCB	0.9 <del>8</del>	1.00	0.87 (0.16)	0.91 (0.05)
JMA	0.9 <del>5</del>	1.00	0.9 <del>9</del> (0.12)	1.00 (0.07)
MATCH:NCEP	0.9 <del>3</del>	0.9 <del>7</del>	1.01 (0.17)	1.11 (0.17)
MATCH:MACCM	0.9 <del>7</del>	0.9 <del>9</del>	0.7 <del>9</del> (0.16)	0.86 (0.05)
NIES	0.9 <del>7</del>	1.00	0.7 <del>9</del> (0.12)	0.86 (0.07)
NIRE	0.9 <del>8</del>	1.00	0.6 <del>5</del> (0.07)	0.73 (0.09)
TM2	0.9 <del>5</del>	0.9 <del>9</del>	0.8 <del>5</del> (0.11)	0.86 (0.08)
TM3	0.9 <del>2</del>	1.00	0.7 <del>6</del> (0.19)	0.91 (0.06)
Model Mean	0.9 <del>8</del>	1.00	0.8 <del>3</del> (0.13)	0.91 (0.08)

Deleted: spo...PO, SYOsy... psa, m... [1]

Cynthia Nevison 10/24/2014 9:24 PM

Formatted ... [2]

Cynthia Nevison 10/24/2014 12:18 PM

Deleted: >-

Cynthia Nevison 10/24/2014 12:18 PM

Deleted: >

Cynthia Nevison 10/24/2014 9:19 PM

Deleted: 8

Cynthia Nevison 10/24/2014 9:19 PM

Deleted: 9

Cynthia Nevison 10/24/2014 9:22 PM

Deleted: 9... (0.212) ... [3]

Cynthia Nevison 10/24/2014 9:20 PM

Deleted: 9

Cynthia Nevison 10/24/2014 9:22 PM

Deleted: 8

Cynthia Nevison 10/24/2014 9:20 PM

Deleted: 8

Cynthia Nevison 10/24/2014 9:22 PM

Deleted: 1.00... (0.123) ... [4]

Cynthia Nevison 10/24/2014 9:20 PM

Deleted: 7

Cynthia Nevison 10/24/2014 9:19 PM

Deleted: 8

Cynthia Nevison 10/24/2014 9:22 PM

Deleted: 8

Cynthia Nevison 10/24/2014 9:20 PM

Deleted: 9

Cynthia Nevison 10/24/2014 9:19 PM

Deleted: 1.00

Cynthia Nevison 10/24/2014 9:22 PM

Deleted: 80... (0.168) ... [5]

Cynthia Nevison 10/24/2014 9:20 PM

Deleted: 9

Cynthia Nevison 10/24/2014 9:21 PM

Deleted: 81... (0.123) ... [6]

Cynthia Nevison 10/24/2014 9:20 PM

Deleted: 9

Cynthia Nevison 10/24/2014 9:21 PM

Deleted: 6... (0.078) ... [7]

Cynthia Nevison 10/24/2014 9:20 PM

Deleted: 8

Cynthia Nevison 10/24/2014 9:19 PM

Deleted: 1...9900 ... [8]

Cynthia Nevison 10/24/2014 9:21 PM

Deleted: 7

Cynthia Nevison 10/24/2014 9:21 PM

Deleted: 7

Cynthia Nevison 10/24/2014 9:21 PM

Deleted: 80... (0.198) ... [9]

Cynthia Nevison 10/24/2014 9:21 PM

Deleted: 9

Cynthia Nevison 10/24/2014 9:21 PM

Deleted: 4... (0.134) ... [10]

**Table S2.** Correlation coefficient R and ratio of standard deviations:  $\sigma_{\text{pre}}/\sigma_{\text{fs}}$ , representing the **pulse-response code (PRC)** vs. **forward simulation (FS)** correlation in the shape and phase and the amplitude ratio, respectively, of the seasonal cycle in APO at 13 selected monitoring sites. The mean and standard deviation (for  $\sigma_{\text{pre}}/\sigma_{\text{fs}}$  in parentheses) among the 9 ATMs participating in the APO Transcom experiment are given.

Station	Code	Lat. °N	Long. °E	Elev. (m)	Obs Years	$R^2$	$\sigma_{\text{pre}}/\sigma_{\text{fs}}$
Alert	ALT	82.5	-62.5	210	1991-2013 SIO	0.99	0.95 (0.12)
Barrow Alaska	BRW	71.3	-156.6	11	1993-2008 PU	0.97	0.96 (0.10)
Cold Bay Alaska	CBA	55.2	-162.7	25	N/A	0.96	0.66 (0.11)
Sable Island Nova Scot.	SBL	43.9	-60.0	5	N/A	0.95	0.77 (0.11)
Ryori, Japan	RYO	39.0	141.8	260	N/A	0.93	0.77 (0.14)
La Jolla CA	LJO	32.9	-117.3	16	N/A	0.96	0.93 (0.19)
Kumukahi HI	KUM	19.5	-154.8	3	N/A	0.95	1.20 (0.17)
Mauna Loa HI	MLO	19.5	-155.6	3397	N/A	0.97	1.22 (0.20)
Samoa	SMO	-14.3	-170.6	42	N/A	0.95	0.78 (0.07)
Amsterdam Island	AMS	-38.0	77.5	150	N/A	1.00	0.88 (0.10)
Cape Grim Tasmania	CGO	-40.7	144.7	5500	N/A	1.00	0.86 (0.14)
Cape Grim Tasmania	CGO	-40.7	144.7	94	N/A	0.99	0.82 (0.08)
Macquarie Island	MQA	-54.5	159.0	12	1997-2007 PU	1.00	0.89 (0.09)
Palmer Antarctica	PSA	-64.9	-64.0	10	1996-2013 SIO	0.97	1.04 (0.14)
Syowa Antarctica	SYO	-69.0	39.6	11	N/A	0.99	0.93 (0.11)

Deleted: ,

Cynthia Nevison 10/24/2014 9:15 PM

Formatted ... [11]

Cynthia Nevison 10/24/2014 9:15 PM

Formatted ... [12]

Cynthia Nevison 10/24/2014 9:15 PM

Formatted ... [13]

Cynthia Nevison 10/24/2014 9:15 PM

Formatted ... [14]

Cynthia Nevison 10/24/2014 9:07 PM

Deleted: 8

Cynthia Nevison 10/24/2014 9:08 PM

Deleted: 8

Cynthia Nevison 10/24/2014 9:15 PM

Formatted ... [15]

Cynthia Nevison 10/24/2014 9:15 PM

Formatted ... [16]

Cynthia Nevison 10/24/2014 9:09 PM

Deleted: 8

Cynthia Nevison 10/24/2014 9:15 PM

Formatted ... [17]

Cynthia Nevison 10/24/2014 9:15 PM

Formatted ... [18]

Cynthia Nevison 10/24/2014 9:09 PM

Deleted: 8

Cynthia Nevison 10/24/2014 9:15 PM

Formatted ... [19]

Cynthia Nevison 10/24/2014 2:36 PM

Deleted: A

Cynthia Nevison 10/24/2014 9:10 PM

Deleted: 7

Cynthia Nevison 10/24/2014 9:15 PM

Formatted ... [20]

Cynthia Nevison 10/24/2014 9:15 PM

Formatted ... [21]

Cynthia Nevison 10/24/2014 9:12 PM

Deleted: 7

Cynthia Nevison 10/24/2014 9:15 PM

Formatted ... [22]

Cynthia Nevison 10/24/2014 9:15 PM

Formatted ... [23]

Cynthia Nevison 10/24/2014 9:15 PM

Formatted ... [24]

Cynthia Nevison 10/24/2014 9:13 PM

Deleted: 1...9900

Cynthia Nevison 10/24/2014 9:15 PM

Formatted ... [25]

Cynthia Nevison 10/24/2014 9:15 PM

Formatted ... [26]

Cynthia Nevison 10/24/2014 9:15 PM

Formatted ... [27]

Cynthia Nevison 10/24/2014 9:13 PM

Deleted: 9

Cynthia Nevison 10/24/2014 9:15 PM

Formatted ... [28]

▲ South Pole	SPO	-90.0	-24.8	2830	<u>1993-2013 SIO</u>	1.00	0.88 (0.11)

Cynthia Nevison 10/24/2014 9:15 PM  
Formatted: Font:10 pt

At most extratropical stations, the  $\sigma_{\text{prc}}/\sigma_{\text{fs}}$  ratios are  $< 1$  in Table S2, suggesting that the Pulse Response Code tends to underestimate the true APO amplitude from the forward simulations. This may be due to the uniform flux distributions assumed across Transcom regions, which could smooth out hotspots for  $\text{O}_2$  air-sea flux that may lead to more intense peaks in true APO. Although the PRC vs. FS comparison is purely model based, the timespan used to compute the observed mean APO seasonal cycle at the 5 selected stations shown in the main text is also listed in Table S2.

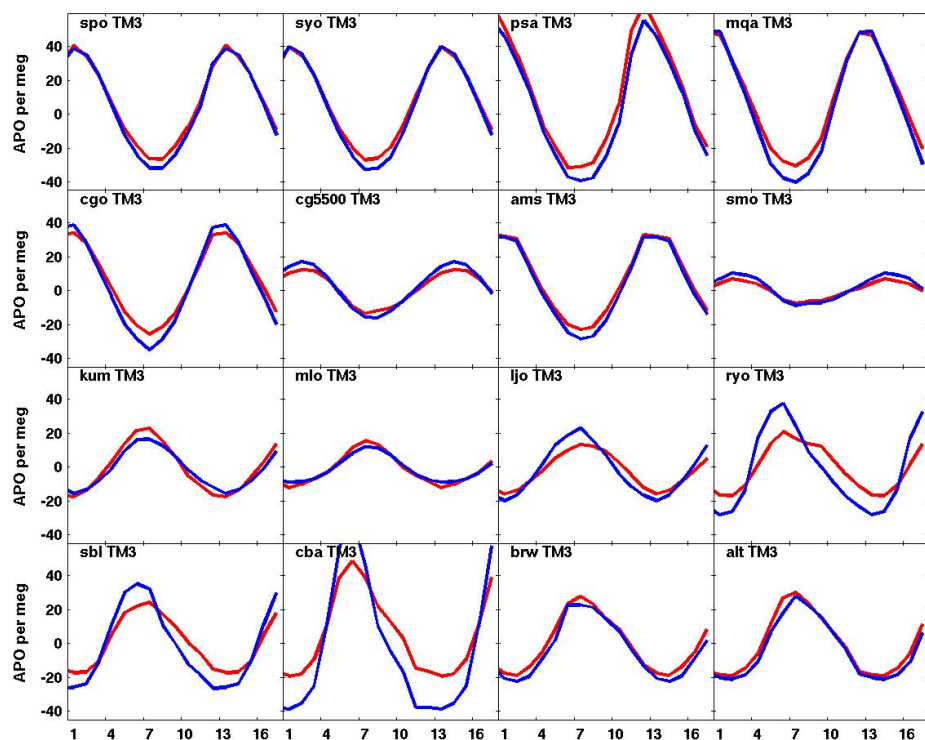


**Figure S1.** Mean seasonal cycle in atmospheric APO produced by forcing the TM3 atmospheric transport model with monthly mean  $O_2$  and  $N_2$  fluxes from the monthly flux climatology of *Garcia and Keeling* [2001]. Archived results from T3L2 **TM3** forward simulations from the APO Transcom experiment (blue) are compared to estimates using the **TM3** variant of the pulse-response code (red) at 16 stations: **SPO** (South Pole), **SYO** (Syowa), **PSA** (Palmer Station), **MQA** (Macquarie), **CGO** (Cape Grim surface), **CGQ5500** (Cape Grim/Bass Strait 5500m), **AMS** (Amsterdam Island), **SMO** (Samoa), **MLQ** (Mauna Loa), **LJO** (La Jolla, California), **RYO** (Ryori), **SBL** (Sable Island, Canada), **CBA** (Cold Bay, Alaska), **BRW** (Barrow, Alaska), **ALT** (Alert, Greenland).

Cynthia Nevison 10/24/2014 1:37 PM

**Deleted:** GCTM

Cynthia Nevison 10/24/2014 1:37 PM

**Deleted:** GCTM

Cynthia Nevison 10/24/2014 1:38 PM

**Deleted:** spo

Cynthia Nevison 10/24/2014 1:38 PM

**Deleted:** syo

Cynthia Nevison 10/24/2014 1:38 PM

**Deleted:** psa

Cynthia Nevison 10/24/2014 1:38 PM

**Deleted:** mqa

Cynthia Nevison 10/24/2014 1:38 PM

**Deleted:** cgo

Cynthia Nevison 10/24/2014 1:38 PM

**Deleted:** cgo

Cynthia Nevison 10/24/2014 1:38 PM

**Deleted:** ams

Cynthia Nevison 10/24/2014 1:39 PM

**Deleted:** smo

Cynthia Nevison 10/24/2014 1:39 PM

**Deleted:** mlo

Cynthia Nevison 10/24/2014 1:39 PM

**Deleted:** ljo

Cynthia Nevison 10/24/2014 1:39 PM

**Deleted:** ryo

Cynthia Nevison 10/24/2014 1:39 PM

**Deleted:** sbl

Cynthia Nevison 10/24/2014 1:39 PM

**Deleted:** cba

Cynthia Nevison 10/24/2014 1:39 PM

**Deleted:** brw

Cynthia Nevison 10/24/2014 1:39 PM

**Deleted:** alt

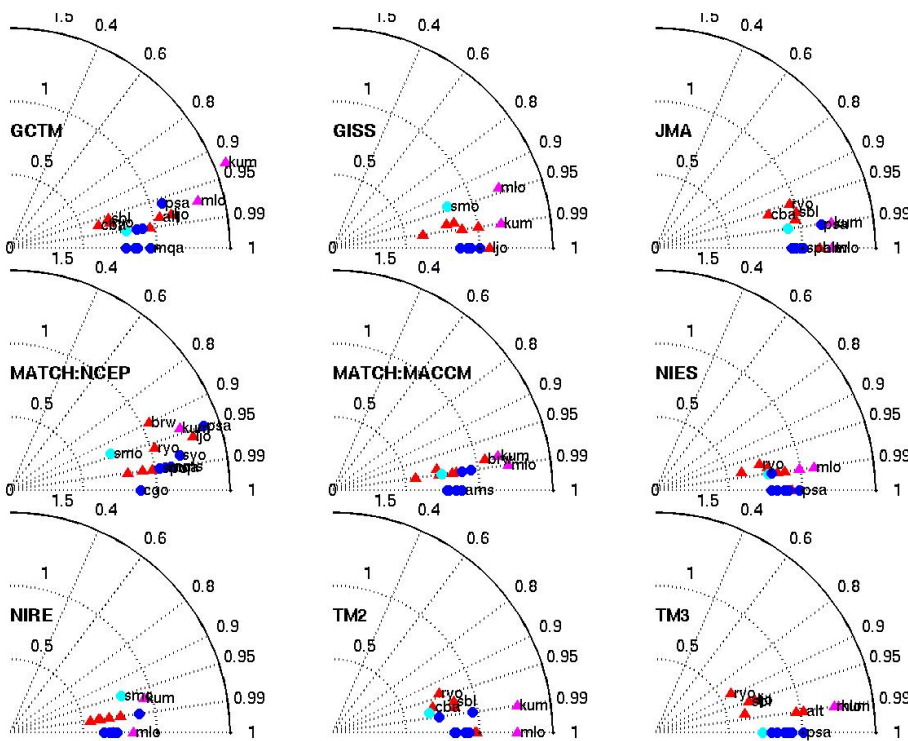
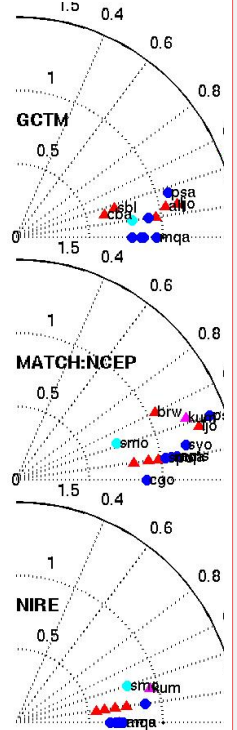


**Figure S2.** Taylor diagrams [Taylor, 2001] illustrating the correlation in phase, shape and amplitude between the pulse-response code and the archived T3L2 forward simulations for the 9 ATMs participating in APO Transcom, forced by monthly mean O<sub>2</sub> and N<sub>2</sub> fluxes from the monthly flux climatology of Garcia and Keeling [2001]. The reference point at a radius (amplitude ratio) of 1 and correlation coefficient (angle) of 1.0 represents perfect agreement with the forward simulation. Each symbol on the Taylor diagram represents one of 16 sampling sites, color coded by latitude (blue = <-25S, cyan=southern tropical, magenta = northern tropical, red = >25N), which are labeled by 3-letter station code where legibility permits.

#### Reference:

Taylor, K. E., 2001, Summarizing multiple aspects of model performance in a single diagram, *J. Geophys. Res.*, 106(D7), 7183–7192.

Cynthia Nevison 10/24/2014 2:34 PM



Deleted:

Unknown

Formatted: Font:Times New Roman

Cynthia Nevison 10/24/2014 1:43 PM

Deleted: agreement

Cynthia Nevison 10/24/2014 1:43 PM

Formatted: Font:Italic

Cynthia Nevison 10/24/2014 2:35 PM

Deleted: 3

Cynthia Nevison 10/24/2014 1:49 PM

Formatted: Font:11 pt

